AD NUMBER

AD862093

NEW LIMITATION CHANGE

TO

Approved for public release, distribution unlimited

FROM

Distribution authorized to U.S. Gov't. agencies and their contractors; Administrative/Operational Use; 9 Oct 1969. Other requests shall be referred to Army Missile Command, Redstone Arsenal, AL.

AUTHORITY

USAMC ltr, 29 Nov 1972

REPORT NO. RE-TR-69-20

OPTIMAL CONTROLLERS FOR HOMING MISSILES WITH TWO TIME CONSTANTS

by

G. C. Willems

October 1969

U.S. ARMY MISSILE COMMAND
Redstone Arsenal, Alabama 35809

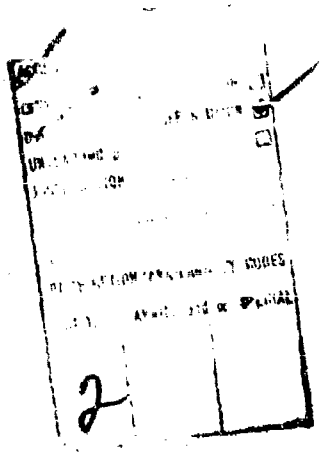

DISCLAIMER

The findings in this report are not to be construed as an official Department of the Army position unless so designated by other authorized documents.

DISPOSITIONS INSTRUCTIONS

Destroy this report when it is no longer needed. Do not return it to the originator.

9 October 1969

Report No. RE-TR-69-20

OPTIMAL CONTROLLERS FOR HOMING MISSILES WITH TWO TIME CONSTANTS

by

G. C. Willems

DA Project No. 1M2623XXA204
AMC Management Structure Code No. 522C.11.146

Advanced Sensors Laboratory
Research and Engineering Directorate (Provisional)
U. S. Army Missile Command
Redstone Arsenal, Alabama 35809

ABSTRACT

Optimum control theory is applied to develop a guidance law for homing missiles for which the airframe dynamics is not neglected. This work extends the applicability of the laws derived in a previous report to systems characterized by two time constants.

The effectiveness of the optimum controller thus derived is evaluated in an example by comparing it with classical proportional navigation. Additionally, extensive quantitative plots of the controller parameters are provided as an aid in specific designs.

ACKNOWLEDGEMENTS

The author wishes to thank C. P. Bailey and W. Anderson of the Advanced Sensors Laboratory, and B. Bergin of the Computation Laboratory, Missile Command for rendering the computer programs. Theirs has been a significant contribution to this project.

CONTENTS

		Page
Section I.	INTRODUCTION	1
Section II.	THE MINIMUM ERROR REGULATOR PROBLEM	2
Section III.	OPTIMUM CONTROLLER FOR A TWO-TIME CONSTANT MISSILE	5
Section IV.	QUANTITATIVE ANALYSIS OF A TYPICAL HOMING SYSTEM	17
1.	Analysis of the Controller Equations	17
2.	Comparative Evaluation of Optimum Controller and Proportional Navigation	17
3.	The Effective Navigation Ratio	25
4.	The Effect of the Parameter λ	29
Section V.	MECHANIZATION CONSIDERATIONS	31
Section VI.	CONCLUSIONS	34
Appendix A.	COMPUTATION OF COMPONENT TERMS OF F(t)	35
Appendix B.	NUMERICAL DATA FOR OPTIMUM CONTROLLER GAINS	39
REFERENCES		57

ILLUSTRATIONS

Table		Page
I	Simulation Parameters	22

Figure		
1	Optimal Control System	3
2	Typical Homing Block Diagram	5
3	Rearranged Homing Block Diagram	6
4	Augmented Homing System	6

ILLUSTRATIONS (Continued)

Figure		Page
5	Simplified Homing Geometry	18
6-a	Block Diagram of Optimum Controller	19
6-b	Controller Modified with $\dot{\Lambda}$ as Input	19
7-a	Simulation Block Diagram for Example System	20
7-b	Adjoint Homing Model	21
8-a	Simulated N Function	23
8-b	Simulated NG_3 Function	23
8-c	Simulated NG_4 Function	25
9	Noise PSD for Example	25
10	Miss Due to Random Heading Disturbances	26
11	Miss Due to Random Disturbance on $\dot{\Lambda}$	26
12	System Response to Wide Band Noise	27
13	Miss Due to Narrow Band Noise	27
14	Miss Due to Narrow Band Noise for Three-Time Constant System	28
15	Miss Due to Random Disturbance on $\dot{\Lambda}$ (System with Three τ's)	28
16	Effect of Varying λ on Miss Due to Random Disturbance on $\dot{\Lambda}$	30
17	Feasible Concept for Approximating N	33
B-1	N Versus t_{go} for $\omega_1 = 0.2$, $\lambda = 0$	40
B-2	N Versus t_{go} for $\omega_1 = 0.33$, $\lambda = 0$	41
B-3	N Versus t_{go} for $\omega_1 = 0.5$, $\lambda = 0$	42
B-4	N Versus t_{go} for $\omega_1 = 1$, $\lambda = 0$	43
B-5	N Versus t_{go} for $\omega_1 = 2$, $\lambda = 0$	44
B-6	N Versus t_{go} for $\omega_1 = 5$, $\lambda = 0$	45
B-7	N Versus t_{go} for $\omega_1 = 0.2$, $\lambda = 1$	46
B-8	N Versus t_{go} for $\omega_1 = 0.33$, $\lambda = 1$	47
B-9	N Versus t_{go} for $\omega_1 = 0.5$, $\lambda = 1$	48
B-10	N Versus t_{go} for $\omega_1 = 1$, $\lambda = 1$	49
B-11	N Versus t_{go} for $\omega_1 = 2$, $\lambda = 1$	50
B-12	N Versus t_{go} for $\omega_1 = 5$, $\lambda = 1$	51
B-13	G_4 Versus t_{go} for $\omega_1 = 0.2$	52
B-14	G_4 Versus t_{go} for $\omega_1 = 0.33$	52

ILLUSTRATIONS (Concluded)

Figure		Page
B-15	G_4 Versus t_{go} for $\omega_1 = 0.5$	53
B-16	G_4 Versus t_{go} for $\omega_1 = 1$	53
B-17	G_4 Versus t_{go} for $\omega_1 = 2$	54
B-18	G_4 Versus t_{go} for $\omega_1 = 5$	54
B-19	G_3 Versus t_{go} for Various Values of ω_2	55

Section I. INTRODUCTION

The technique of proportional navigation (PN) has been found to be the most satisfactory method of guiding homing missiles — a fact established by engineers through many years of design experience rather than by analytical proof. In PN, an attempt is made to mechanize the following equation:

$$\dot{\gamma} = N\dot{\Lambda}; \qquad 2 < N \leq 5 ,$$

where $\dot{\gamma}$ is the missile angular turning rate and $\dot{\Lambda}$ is the line-of-sight angular rate referred to inertial space. N is denoted as the "navigation ratio," and again, the range of acceptable values has been developed mainly through experience. It is interesting to note that recently it has been rigorously determined by means of modern control theory that PN is indeed optimal in that for unconstrained control effort, the miss distance at intercept is minimized in the mean-squared sense. The correspondence between PN and optimum control (OC) has been demonstrated by Bryson, Ho, and Baron [1], Janus [2], and Speyer [3], among others.

A previous report [4] verified the optimality of PN by casting the problem as a "minimum error regulator" problem and using the Ogata [5] method of solution. The weakness of the cited work in OC, as well as the classical derivation of PN, is that the plant (missile) is assumed to respond instantaneously to guidance commands, i.e., has no time lags. The previous report [4] extended prior work by deriving the OC for a missile having a single time constant. It was shown that the addition of the time lag profoundly affects the steering law in that the OC for this case requires time varying gains. These results point out that missile dynamics should not be neglected if realistic OC's are to be obtained.

Typical homing missiles cannot realistically be characterized by a single time constant; two or even three lags are required for adequate modeling. The purpose of this study is to derive the OC for a two-time constant system, and to analyze the performance of this controller relative to conventional PN. The effect of using such a controller in a system characterized by three time constants will also be investigated; it is conjectured that, although, it is suboptimal for this case, such a scheme would nevertheless be superior to PN, since the latter takes no time lags into account. The method of solution used is to cast the problem in a form such that the Ogata method, which has been described and verified [4], can be used.

Section II. THE MINIMUM ERROR REGULATOR PROBLEM

Any linear dynamical system of the n^{th} order can be expressed either as an n^{th} order differential equation or a set of n first-order differential equations. The latter is known as the state formulation and is used herein, since it lends itself to matrix-vector notation and manipulation. It will be assumed that the system differential equation is given by:

$$\dot{x} = Ax + Bu; \qquad x(0) = C \ ,$$

where

x = n dimensional column state vector

u = r dimensional control vector

A = n × n matrix

B = n × r matrix

and where the following index is to be minimized:

$$J(C,T) = \underbrace{x^*(T)Px(T)}_{\substack{\text{Terminal}\\ \text{state}\\ \text{weighting}}} + \int_0^T \underbrace{x^*(t)Qx(t)dt}_{\substack{\text{State}\\ \text{weighting}}} + \int_0^T \underbrace{u^*(t)R(t)u(t)dt}_{\text{Control cost}} \ .$$

The * symbol denotes the conjugate transpose of the vector, or simply the transpose for real vectors, and P, Q(t), R(t) are matrices of appropriate dimensions.

Ogata shows that the optimum controller for such a system can be obtained by solving the nonhomogeneous matrix Riccati equation:

$$\frac{dS}{dt} = -SA - A^*S + SBR^{-1}(0)B^*S = Q(0) \ .$$

If the matrices A and B are constant, i.e., if the system is stationary, the above matrix equation can be solved in closed form for the time T:

$$S(T) = \{[\phi_{21}(T) + \phi_{22}(T)P][\phi_{11}(T) + \phi_{12}(T)P]^{-1}\} \ ,$$

where the ϕ_{ij} are obtained from partitioning the matrix

$$e^{MT} \triangleq \left[\begin{array}{c|c} \phi_{11}(T) & \phi_{12}(T) \\ \hline \phi_{21}(T) & \phi_{22}(T) \end{array}\right]$$

and M is defined as

$$M = \left[\begin{array}{c|c} -A & BR^{-1}(0)B^* \\ \hline Q(0) & A^* \end{array}\right] ,$$

from which it can be seen that M is known from the problem statement and the performance index.

Once S(T) is known, the optimum control vector can be obtained from the expression

$$u_{opt}(t) = -F(T-t)x(t) ,$$

where

$$F(T-t) = R^{-1}(t)B^*S(T-t) .$$

In block diagram form, the OC can be depicted as in Figure 1.

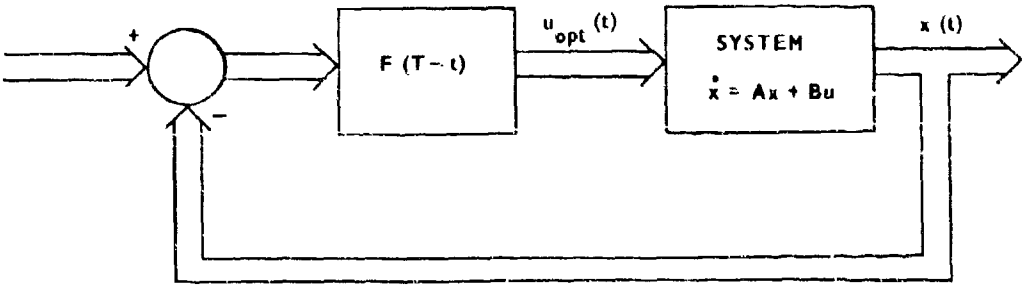

FIGURE 1. OPTIMAL CONTROL SYSTEM

The solution of the subject problem can then be summarized as follows:

1) From system state equations, and the given performance index, the following matrices are known:

$$A,\ B,\ P,\ Q,\ R$$

2) The matrix M can be formed from above

$$M = \left[\begin{array}{c|c} -A & BR^{-1}(0)B^* \\ \hline Q(0) & A^* \end{array}\right] .$$

3) From knowledge of M, e^{MT} can be found. There are several methods for computing this, but the use of the Laplace transform is often the most convenient. This method involves the relationship

$$\mathcal{L}\left[e^{MT}\right] = [sI - M]^{-1} ,$$

where s is the Laplace operator and I the unit matrix.

4) Once e^{MT} is known, all of the ϕ_{ij} are obtained from the relation

$$e^{MT} = \left[\begin{array}{c|c} \phi_{11}(T) & \phi_{12}(T) \\ \hline \phi_{21}(T) & \phi_{22}(T) \end{array}\right] .$$

From this, S(T) can be computed:

$$S(T) = \{[\phi_{21}(T) + \phi_{22}(T)P][\phi_{11}(T) + \phi_{12}(T)P]^{-1}\} .$$

5) Once S(T) is known, $u_{opt}(t)$ and F(T - t) are immediately obtainable:

$$F(T - t) = R^{-1}(t)B^*S(T - t)$$

$$u_{opt}(t) = F(T - t)x(t) .$$

The optimum system thus mechanized will minimize the given quadratic index in the solution interval $0 \leq t \leq T$. It should be noted that the optimum solution is given in terms of time-to-go (T - t) rather than elapsed time t.

Section III. OPTIMUM CONTROLLER FOR A TWO-TIME CONSTANT MISSILE

The conventional overall loop can be depicted as shown in Figure 2 and can be readily rearranged with target acceleration $\left(\ddot{y}_t\right)$ as an input in the manner of Figure 3. By assuming two time constants for the dynamic lag of the missile-autopilot combination, the model of Figure 4 is obtained. This figure also includes an exponential decay model for target acceleration, to the left of the dashed line in Figure 4. The contribution of the target acceleration has, however, been previously computed [4] and, since it remains invariant with the order of the plant, it does not need to be explicitly considered herein. With reference to Figure 4, the problem can be stated as follows: Given the observable states x_1, x_2, x_3, and x_4, the control vector is determined that will minimize the miss distance at intercept only, i.e.,

$$y_d(t)\Big|_{t=T} = \text{minimum in the mean squared sense subject to a constraint on available control effort.}$$

The state equations can be written directly from Figure 4; the target acceleration term is ignored for now and will be appended later, since it is the same as for the cases previously treated.

$$\dot{x}_1 = x_2$$
$$\dot{x}_2 = -g\, x_3$$
$$\dot{x}_3 = -\omega_2 x_3 + \omega_2 x_4$$
$$\dot{x}_4 = -\omega_1 x_4 + \omega_1 n_c \ .$$

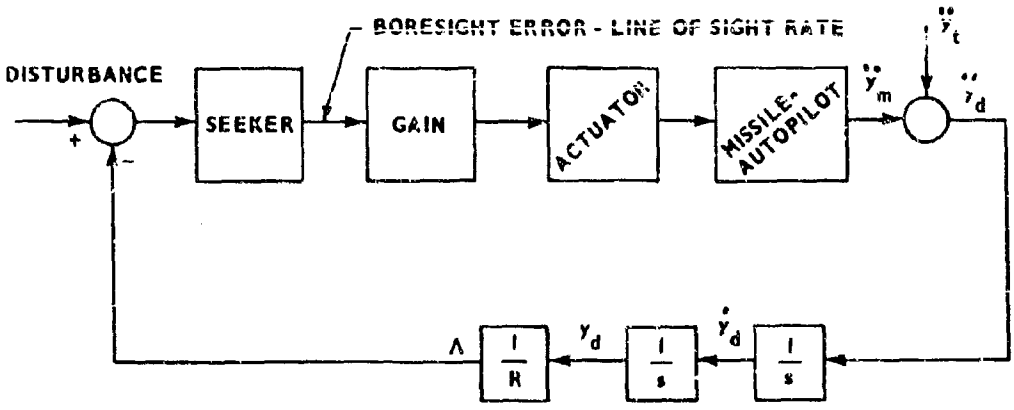

FIGURE 2. TYPICAL HOMING BLOCK DIAGRAM

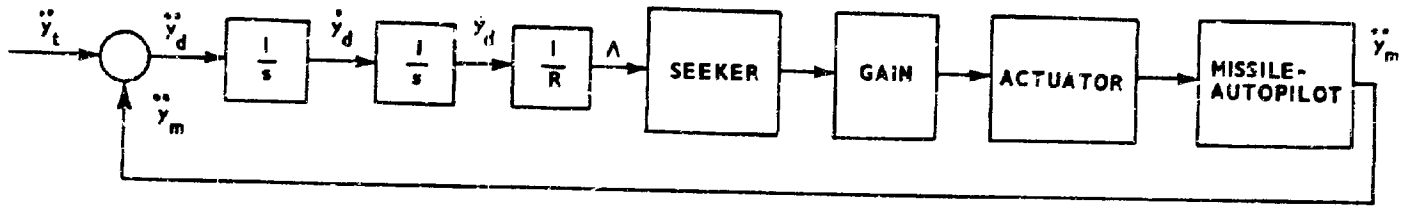

FIGURE 3. REARRANGED HOMING BLOCK DIAGRAM

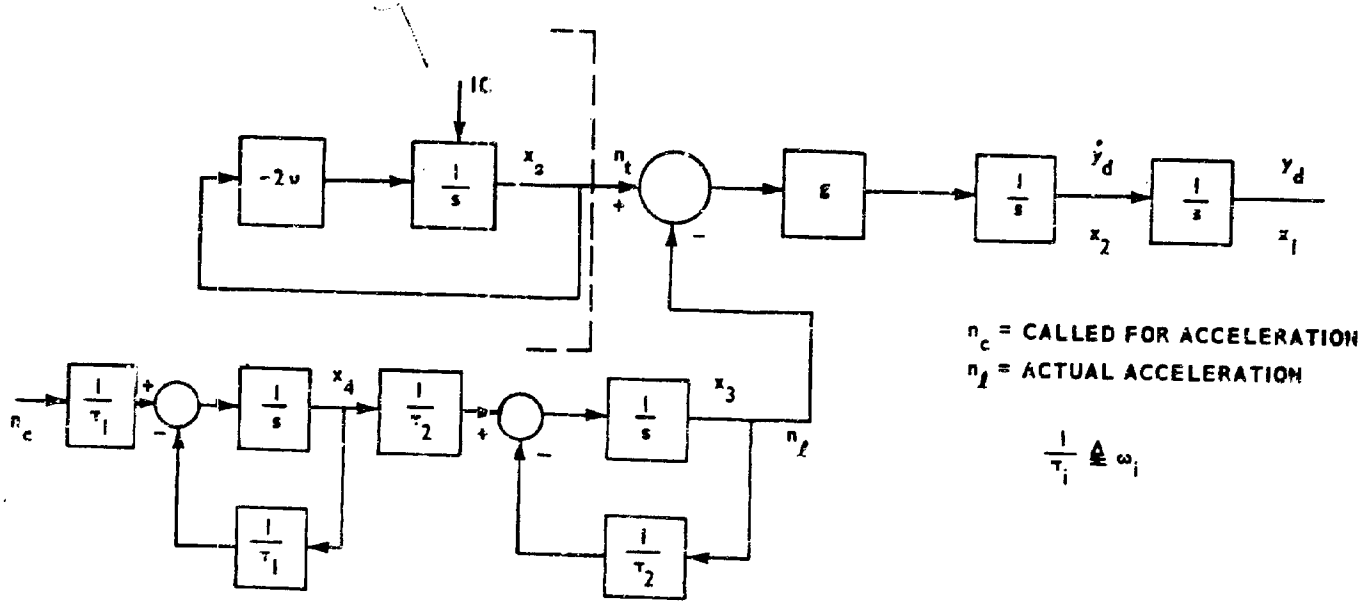

FIGURE 4. AUGMENTED HOMING SYSTEM

In the vector-matrix form, these become

$$\begin{bmatrix} \dot{x}_1 \\ \dot{x}_2 \\ \dot{x}_3 \\ \dot{x}_4 \end{bmatrix} = \begin{bmatrix} 0 & 1 & 0 & 0 \\ 0 & 0 & -g & 0 \\ 0 & 0 & -\omega_2 & \omega_2 \\ 0 & 0 & 0 & -\omega_1 \end{bmatrix} \begin{bmatrix} x_1 \\ x_2 \\ x_3 \\ x_4 \end{bmatrix} + \begin{bmatrix} 0 \\ 0 \\ 0 \\ \omega_1 \end{bmatrix} n_c \quad .$$

The generalized index J

$$J = x^*(T)Px(T) + \int_0^T [x^*(t)Q(t)x(t) + u^*(t)R(t)u(t)]dt$$

is reduced to the desired form by defining

$$P = \begin{bmatrix} 1 & 0 & 0 & 0 \\ 0 & 0 & 0 & 0 \\ 0 & 0 & 0 & 0 \\ 0 & 0 & 0 & 0 \end{bmatrix}; \quad Q = [0]_{4 \times 4}; \quad R = \lambda = \text{scalar}$$

which yields the form

$$J = x_1(T)^2 + \lambda \int_0^T n_c{}^2 dt \quad .$$

The above index minimizes only y_d at intercept as desired. The matrix M is obtained next:

$$M = \left[\begin{array}{cccc|cccc} 0 & -1 & 0 & 0 & 0 & 0 & 0 & 0 \\ 0 & 0 & g & 0 & 0 & 0 & 0 & 0 \\ 0 & 0 & \omega_2 & -\omega_2 & 0 & 0 & 0 & 0 \\ 0 & 0 & 0 & \omega_1 & 0 & 0 & 0 & \frac{\omega_1^2}{\lambda} \\ \hline 0 & 0 & 0 & 0 & 0 & 0 & 0 & 0 \\ 0 & 0 & 0 & 0 & 1 & 0 & 0 & 0 \\ 0 & 0 & 0 & 0 & 0 & -g & -\omega_2 & 0 \\ 0 & 0 & 0 & 0 & 0 & 0 & \omega_2 & -\omega_1 \end{array}\right] ,$$

from which [sI - M] can be formed:

$$[sI - M] = \begin{bmatrix} s & 1 & 0 & 0 & 0 & 0 & 0 & 0 \\ 0 & s & -g & 0 & 0 & 0 & 0 & 0 \\ 0 & 0 & s - \omega_2 & \omega_2 & 0 & 0 & 0 & 0 \\ 0 & 0 & 0 & s - \omega_1 & 0 & 0 & 0 & -\frac{\omega_1^2}{\lambda} \\ 0 & 0 & 0 & 0 & s & 0 & 0 & 0 \\ 0 & 0 & 0 & 0 & -1 & s & 0 & 0 \\ 0 & 0 & 0 & 0 & 0 & g & s + \omega_2 & 0 \\ 0 & 0 & 0 & 0 & 0 & 0 & -\omega_2 & s + \omega_1 \end{bmatrix}$$

Since the above matrix is almost triangular, it is most easily inverted by reducing the augmented matrix,

$$[sI - M \,\vdots\, I] ,$$

to the upper triangular form. The inverse is obtained by solving the triangular matrix as a set of algebraic equations using each column of the augmented section in turn. This process yields the matrix $[sI - M]^{-1}$ as shown:

$$[sI - M]^{-1} = \left[\begin{array}{cccc|c} \frac{1}{s} & -\frac{1}{s^2} & \frac{-g}{s^2(s-\omega_2)} & \frac{g\,\omega_2}{s^2(s-\omega_1)(s-\omega_2)} & \frac{-g^2\,\omega_1^2\,\omega}{\lambda s^1(s-\omega_1)(s+\omega_1)(s} \\ 0 & \frac{1}{s} & \frac{g}{s(s-\omega_2)} & \frac{-g\,\omega_2}{s(s-\omega_1)(s-\omega_2)} & \frac{g^2\,\omega_1^2\,\omega_2}{\lambda s^3(s-\omega_1)(s+\omega_2)(s} \\ 0 & 0 & \frac{1}{s-\omega_2} & \frac{-\omega_2}{(s-\omega_1)(s-\omega_2)} & \frac{g\,\omega_1^2\,\omega_2}{\lambda s^2(s-\omega_1)(s+\omega_1)(s} \\ 0 & 0 & 0 & \frac{1}{(s-\omega_1)} & \frac{-g\,\omega_1^2\,\omega_2}{\lambda s^2(s-\omega_1)(s+\omega_1)(s} \\ \hline 0 & 0 & 0 & 0 & \frac{1}{s} \\ 0 & 0 & 0 & 0 & \frac{1}{s^2} \\ 0 & 0 & 0 & 0 & \frac{-g}{s^2(s+\omega_2} \\ 0 & 0 & 0 & 0 & \frac{-g\,\omega_2}{s^2(s+\omega_1)(s} \end{array}\right]$$

$\frac{g^2\,\omega_1^2\,\omega_2^2}{(s+\omega_1)\,(s-\omega_2)\,(s+\omega_2)}$	$\frac{-\,g^2\,\omega_1^2\,\omega_2^2}{\lambda s^3\,(s-\omega_1)\,(s+\omega_1)\,(s-\omega_2)\,(s+\omega_2)}$	$\frac{g\,\omega_1^2\,\omega_2^2}{\lambda s^2\,(s-\omega_1)\,(s+\omega_1)\,(s-\omega_2)\,(s+\omega_2)}$	$\frac{g\,\omega_1^2\,\omega_2}{\lambda s^2\,(s-\omega_1)\,(s+\omega_1)\,(s-\omega_2)}$
$\frac{g^2\,\omega_1^2\,\omega_1^2}{(s+\omega_2)\,(s-\omega_2)\,(s+\omega_2)}$	$\frac{g^2\,\omega_1^2\,\omega_2^2}{\lambda s^2\,(s-\omega_1)\,(s+\omega_1)\,(s-\omega_2)\,(s+\omega_2)}$	$\frac{-\,g\,\omega_1^2\,\omega_2^2}{\lambda s\,(s-\omega_1)\,(s+\omega_1)\,(s-\omega_2)\,(s+\omega_2)}$	$\frac{-\,g\,\omega_1^2\,\omega_2}{\lambda s\,(s-\omega_1)\,(s+\omega_1)\,(s-\omega_2)}$
$\frac{g\,\omega_1^2\,\omega_2^2}{(s+\omega_1)\,(s-\omega_2)\,(s+\omega_2)}$	$\frac{g\,\omega_1^2\,\omega_2^2}{\lambda s\,(s-\omega_1)\,(s+\omega_1)\,(s-\omega_2)\,(s+\omega_2)}$	$\frac{-\,\omega_1^2\,\omega_2^2}{\lambda\,(s-\omega_1)\,(s+\omega_1)\,(s-\omega_2)\,(s+\omega_2)}$	$\frac{-\,\omega_1^2\,\omega_2}{\lambda\,(s-\omega_1)\,(s+\omega_1)\,(s-\omega_2)}$
$\frac{\omega_1^2\,\omega_2}{(s+\omega_1)\,(s+\omega_2)}$	$\frac{-\,g\,\omega_1^2\,\omega_2}{\lambda s\,(s-\omega_1)\,(s+\omega_1)\,(s+\omega_2)}$	$\frac{\omega_1^2\,\omega_2}{\lambda\,(s-\omega_1)\,(s+\omega_1)\,(s+\omega_2)}$	$\frac{\omega_1^2}{\lambda\,(s-\omega_1)\,(s+\omega_1)}$

$\frac{1}{s}$	0	0	0
$\frac{1}{s^2}$	$\frac{1}{s}$	0	0
$\frac{-\,g}{s^2\,(s+\omega_2)}$	$\frac{-\,g}{s\,(s+\omega_2)}$	$\frac{1}{s+\omega_2}$	0
$\frac{-\,g\,\omega_2}{(s+\omega_1)\,(s+\omega_2)}$	$\frac{-\,g\,\omega_2}{s\,(s+\omega_1)\,(s+\omega_2)}$	$\frac{\omega_2}{(s+\omega_1)\,(s+\omega_2)}$	$\frac{1}{s+\omega_1}$

Correctness of this matrix can be verified by multiplying it by [sI - M] and observing that the unit matrix results. The ϕ_{ij} needed for the compilation of S(t) are now available, since

$$[sI - M]^{-1} = \begin{bmatrix} \phi_{11}(s) & \phi_{12}(s) \\ \phi_{21}(s) & \phi_{22}(s) \end{bmatrix} .$$

The computation of S(t) requires the computation of the following two matrices:

$$[\phi_{21}(t) + \phi_{22}(t)P]$$
$$[\phi_{11}(t) + \phi_{12}(t)P]^{-1} .$$

Since P is a number matrix, and the addition operation is invariant in the inverse Laplace transformation, the terms within the brackets can be computed prior to determining the inverse transform of the ϕ_{ij}. Also, not all of the terms of each ϕ_{ij} will be needed; therefore, the matrix elements will be denoted symbolically. This reduces computational complexity considerably. The matrix $\phi_{21}(t)$ is the null matrix; therefore the quantity $[\phi_{21}(t) + \phi_{22}(t)P]$ is merely the transform of the first column of $\phi_{22}(s)$, to be denoted symbolically as

$$[\phi_{21}(t) + \phi_{22}(t)P] = \begin{bmatrix} h & 0 & 0 & 0 \\ i & 0 & 0 & 0 \\ j & 0 & 0 & 0 \\ k & 0 & 0 & 0 \end{bmatrix} .$$

The form of $[\phi_{11} + \phi_{12}P]$ is

$$\phi_{11} + \phi_{12}P = \begin{bmatrix} a_{11} & a_{12} & a_{13} & a_{14} \\ a_{21} & a_{22} & a_{23} & a_{24} \\ a_{31} & 0 & a_{33} & a_{34} \\ a_{41} & 0 & 0 & a_{44} \end{bmatrix} .$$

Inversion by partitioning into 2 × 2 matrices is simplest in this case; given a matrix

$$s = \left[\begin{array}{c|c} A & B \\ \hline C & D \end{array}\right]$$

and its inverse

$$s^{-1} = \left[\begin{array}{c|c} \frac{K}{M} & \frac{L}{N} \end{array}\right] .$$

The relationship between the two matrices can be established with the aid of the auxiliary relations,

$$[s^{-1}s] = [s\, s^{-1}] = I$$

which yield the equations

$$K = (A - BD^{-1}C)^{-1} \qquad L = -K\,B\,D^{-1}$$

$$M = -D^{-1}\,C\,K \qquad N = -D^{-1} - D^{-1}\,C\,L .$$

The application of the above formulas to the symbolic representation of $[\phi_{11} + \phi_{12}P]$ yields the desired inverse:

$$[\phi_{11} + \phi_{12}P]^{-1} = \frac{1}{C_1}\begin{bmatrix} a_{22}a_{33}a_{44} - a_{12}a_{23}a_{44} - a_{22}a_{13}a_{44} + a_{12}a_{23}a_{44} - a_{14}a_{22}a_{33} + a_{13}a_{34}a_{22} - a_{34}a_{23}a_{12} + a_{12}a_{24}a_{33} \\ --- \quad --- \quad --- \quad --- \\ --- \quad --- \quad --- \quad --- \\ --- \quad --- \quad --- \quad --- \end{bmatrix}$$

where

$$C_1 = (a_{11}a_{22}a_{33}a_{44} - a_{21}a_{13}a_{44}a_{32} + a_{22}a_{13}a_{34}a_{41} - a_{22}a_{14}a_{41}a_{33} - a_{12}a_{21}a_{33}a_{44}$$

$$+ a_{12}a_{23}a_{44}a_{31} - a_{12}a_{34}a_{23}a_{41} + a_{12}a_{24}a_{33}a_{41}) .$$

It will be shown that only the first row of $[\phi_{11} + \phi_{12}P]^{-1}$ is needed. For this reason, the remaining rows were not computed. The matrix $S(t)$ can now be computed since $S(t) = [\phi_{21} + \phi_{22}P]\,[\phi_{11} + \phi_{12}P]^{-1}$;

$$S(t) = \frac{1}{C_1}\begin{bmatrix} h\,K_1 & h\,K_2 & h\,K_3 & h\,K_4 \\ i\,K_1 & i\,K_2 & i\,K_3 & i\,K_4 \\ j\,K_1 & j\,K_2 & j\,K_3 & j\,K_4 \\ k\,K_1 & k\,K_2 & k\,K_3 & k\,K_4 \end{bmatrix} ,$$

where

$$K_1 = a_{22}a_{33}a_{44}$$

$$K_2 = -a_{12}a_{33}a_{44}$$

$$K_3 = -a_{22}a_{13}a_{44} + a_{12}a_{23}a_{44}$$

$$K_4 = -a_{14}a_{22}a_{33} + a_{13}a_{34}a_{22} - a_{34}a_{23}a_{12} + a_{12}a_{24}a_{33}\,.$$

Finally, the optimum controller can now be written from the previously stated formula $F(T-t) = R^{-1}B^{*}S(T-t)$

$$F(T-t) = \frac{\omega_1^2 k}{\lambda C_1} \left[K_1\ K_2\ K_3\ K_4\right]_{t\,=\,(T-t)\,=\,t_{go}}$$

and

$$u_{opt}\left(t_{go}\right) = -\,F\left(t_{go}\right)x(t)\ .$$

The remaining task consists of obtaining the quantities k, C_1, K_1, K_2, K_3, and K_4 as a function of the specific problem variables; for the subject problem this is algebraically an onerous task. The first step consists of finding the a_{ij} and k by inverse Laplace transforming the elements of $(\phi_{11} + \phi_{12}P)$. The details of this computation are relegated to Appendix A. Knowledge of the values of k and the a_{ij} allows C_1 and the K_i, and consequently, $F(t)$ to be computed. By omitting the algebraic details, ($t = t_{go}$ is implied)

$$\frac{\omega_1^2\,k}{\lambda\,C_1} = \frac{-\,g\left[\omega_1 t - \left(\frac{\omega_1+\omega_2}{\omega_2}\right) - \frac{\omega_2\,e^{-\omega_1 t}}{\omega_1-\omega_2} + \frac{\omega_1^2\,e^{-\omega_2 t}}{\omega_2(\omega_1-\omega_2)}\right]}{e^{(\omega_1+\omega_2)t}\left[\lambda + g^2\,\omega_1\,(I)\right]}$$

is obtained, where

$$I = \left[\frac{2(\omega_2 t-1)}{\omega_1^2(\omega_1-\omega_2)}\,e^{-\omega_1 t} - \frac{2(\omega_1 t-1)}{\omega_2^2(\omega_1-\omega_2)}\,e^{-\omega_2 t}\right.$$

$$\frac{-\,\omega_2^2}{2\omega_1^3(\omega_1-\omega_2)^2}\,e^{-2\omega_1 t} - \frac{\omega_1^2}{2\omega_2^3(\omega_1-\omega_2)^2}\,e^{-2\omega_2 t} + \frac{2}{(\omega_1^2-\omega_2^2)(\omega_1-\omega_2)}\,e^{-\omega_1 t}e^{-\omega_2 t}$$

$$\left. + \frac{\omega_1^2}{2\omega_2^3(\omega_1^2-\omega_2^2)} - \frac{\omega_2^2}{2\omega_1^3(\omega_1^2-\omega_2^2)} - \frac{(\omega_1+\omega_2)(\omega_1 t-1)(\omega_2 t-1)}{\omega_1^2\,\omega_2^2} + \frac{t^3}{3}\right]$$

$$K_1 = e^{(\omega_1 + \omega_2)t}$$

$$K_2 = t\, e^{(\omega_1 + \omega_2)t}$$

$$K_3 = g\, e^{(\omega_1 + \omega_2)t} \left[\frac{1}{\omega_2^2} - \frac{t}{\omega_2} - \frac{e^{-\omega_2 t}}{\omega_2^2} \right]$$

$$K_4 = g\, e^{(\omega_1 + \omega_2)t} \left[\frac{\omega_1^2 \left(1 - \omega_2 t - e^{-\omega_2 t}\right)}{\omega_1^2\, \omega_2\, (\omega_1 - \omega_2)} - \frac{\omega_2^2 \left(1 - \omega_1 t - e^{-\omega_1 t}\right)}{\omega_1^2 \omega_2\, (\omega_1 - \omega_2)} \right] .$$

Cancellation of the common $e^{-(\omega_1 + \omega_2)t}$ term and rearrangement of the remaining terms results in the form

$$F\left(t_{j+1}\right) = - N \left[G_1\, G_2\, G_3\, G_4 \right] ,$$

where

$$N = \frac{g^2 t^2 \left[\omega_1 t - \left(\frac{\omega_1 + \omega_2}{\omega_2} \right) - \frac{\omega_2}{\omega_1 - \omega_2} e^{-\omega_1 t} + \frac{\omega_1^2}{\omega_2 (\omega_1 - \omega_2)} e^{-\omega_2 t} \right]}{\lambda + g^2 \omega_1 (I,}$$

and

$$G_1 = \frac{1}{g\, t^2}$$

$$G_2 = \frac{1}{g\, t}$$

$$G_3 = - \frac{1}{\omega_2^2} \left(\frac{\omega_2\, t\, e^{\omega_2 t} - e^{\omega_2 t} + 1}{e^{\omega_2 t}\, t^2} \right)$$

$$G_4 = - \frac{\omega_2}{\omega_1 - \omega_2} \left[\frac{1}{\omega_1^2} \left(\frac{\omega_1 t\, e^{\omega_1 t} - e^{\omega_1 t} + 1}{e^{\omega_1 t}\, t^2} \right) - \frac{1}{\omega_2^2} \left(\frac{\omega_2 t\, e^{\omega_2 t} - e^{\omega_2 t} + 1}{e^{\omega_2 t}\, t^2} \right) \right] .$$

It is interesting to note that the terms G_1, G_2, and G_3 are identical to the three equivalent terms obtained for the one-time constant system [4]. It should also be noted that the terms of G_3 and G_4 within the parentheses are all identical in form. This is significant in that the same algorithm can be used to compute these terms.

The equations for N and G_4 are not valid for $\omega_1 = \omega_2$, since the term $(\omega_1 - \omega_2)$ becomes zero. This difficulty is resolved by computing a new set of equations for those terms valid only for the case where $\omega_1 = \omega_2$. By appropriately combining the terms of N and G_4, the elements containing $(\omega_1 - \omega_2)$ can be isolated into the indeterminate form 0/0 when $\omega_1 = \omega_2$. L'Hospital's rule can then be

applied, where the differentiation is performed with respect to either ω_1 or ω_2. With the indeterminacies removed, the substitution

$$\omega_1 = \omega_2 = \omega$$

is made into the resulting equation. Application of this technique results in the equation

$$N_{(\omega_1 = \omega_2)} = \frac{g^2 t^2 \left(\omega t - 2 + \omega t\, e^{-\omega t} + 2 e^{-\omega t}\right)}{\lambda + g^2 \omega I_{(\omega_1 = \omega_2)}} .$$

where

$$I_{(\omega_1=\omega_2)} = \left[\frac{t^3}{3} - \frac{3}{4\omega^3} - \frac{2t^2 e^{-\omega t}}{\omega} - \frac{4te^{-\omega t}}{\omega^2} + \frac{4e^{-\omega t}}{\omega^3} - \frac{t^2 e^{-2\omega t}}{2\omega} - \frac{5te^{-2\omega t}}{2\omega^2} - \frac{13e^{-2\omega t}}{4\omega^3} - \frac{2t^2}{\omega} + \frac{4t}{\omega^2}\right]$$

$$G_{4\,(\omega_1 = \omega_2)} = -\frac{1}{\omega^2}\left[\left(\frac{2 + \omega t\, e^{\omega t} - 2e^{\omega t}}{e^{\omega t}\, t^2}\right) + \frac{\omega\, e^{-\omega t}}{t}\right] .$$

We now have equations that are valid for all ω_1. If ω_2 is allowed to approach infinity, i.e., the second time lag is eliminated, the above equations should and do reduce to the ones previously derived [4] for the single lag system.

The optimum controller can now be written

$$u_{opt} = n_c = N\,[G_1\ G_2\ G_3\ G_4] \begin{bmatrix} x_1 \\ x_2 \\ x_3 \\ x_4 \end{bmatrix}$$

or

$$n_c = N\,[G_1 x_1 + G_2 x_2 + G_3 x_3 + G_4 x_4] .$$

However, it is seen (Figure 4) that $x_1 = y_d$ and $x_2 = \dot{y}_d$. Therefore, in terms of these parameters, and the derived values of G_1 and G_2, n_c can be rewritten

$$n_c = N\left(\frac{y_d}{g\, t_{go}^{\,2}} + \frac{\dot{y}_d}{g\, t_{go}}\right) + N\, G_3\, x_3 + N\, G_4\, x_4 .$$

The reason for this representation is that y_d and $\dot{y}_d$ are not usually explicitly measured, since conventional seekers measure the line-of-sight rate $\dot{\lambda}$; since

$\Lambda = y_d/R$, where R is the missile-target range, the following relationship holds:

$$\dot{\Lambda} = \frac{1}{V_c t_{go}} \left(\dot{y}_d + \frac{y_d}{t_{go}} \right) ,$$

where

V_c = closing velocity = $-\dot{R}$.

By use of the above, the control equation can be rewritten

$$n_c = \frac{NV_c}{g} \dot{\Lambda} + NG_3 x_3 + NG_4 x_4 \quad .$$

The first term on right side of above equation is recognized as being analogous to classical PN, except that N is time-varying instead of fixed. The optimum controller also has two additional feedback components from the states x_3 and x_4.

The inclusion of the target acceleration model of Figure 4 requires one additional term in the control equation, the latter having been derived [4]. The controller would take the form

$$n_c = \frac{NV_c}{g} \dot{\Lambda} + NG_3 x_3 + NG_4 x_4 + NG_5 x_5 ,$$

where

$$G_5 = \frac{1}{4\nu^2} \left(\frac{2\nu t_{go} e^{2\nu t_{go}} - e^{-2\nu t_{go}} + 1}{e^{2\nu t_{go}} t_{go}^2} \right)$$

and

$$x_5 = n_t \ .$$

Again it is noted that G_5 has the same form as G_3 and the components of G_4.

All of the analytical parameters required to construct the optimum controller have been obtained. In the next section a quantitative study of a system using such a controller will be performed.

Section IV. QUANTITATIVE ANALYSIS OF A TYPICAL HOMING SYSTEM

1. Analysis of the Controller Equations

The optimum homing system requires computation of N, G_3 and G_4. At first glance this appears to be a formidable task since these quantities are elaborate functions of t_{go}, ω_1, and ω_2. However, for a given missile, ω_1 and ω_2 would remain relatively constant, at least for a limited altitude band; in this study they will be assumed to be constant and the required functions thus become dependent only on t_{go} for a given case. The more general case of varying ω_1 and ω_2 will be discussed later.

Due to their complexity, it is in most instances impractical to compute the required parameters in real time from the given equations. A search for simpler mechanizations requires first that the nature of the subject functions be studied. For this purpose, values of N, G_3 and G_4 have been computed for a wide range of values of ω_1 and ω_2 by using a digital program. Plots of these functions are shown in Appendix B. It is seen that, although they originate from complex equations, the plots of N, G_3 and G_4 show these quantities to be well behaved, continuous functions of t_{go}. Thus, for a given configuration where ω_1 and ω_2 are constants, these quantities could be easily generated as functions of t_{go} by analog (diode function generator) or digital (read-only memory) techniques.

2. Comparative Evaluation of Optimum Controller and Proportional Navigation

The increased complexity of the OC over PN indicates that to be feasible the OC must yield a considerable payoff over PN in terms of reduced miss distance. For this reason, a comparative evaluation using simulation techniques was performed on a simple model, using both the OC and PN concepts.

The sample problem concerns a small homing missile in a low-altitude air-to-ground engagement, with the target assumed stationary. The pertinent geometry is depicted in Figure 5. The model of Figure 4 with the OC appended can be formally represented as shown in Figure 6-a. However, since conventional seekers measure $\dot{\lambda}$, a more convenient representation is that of Figure 6-b. This model was used to generate two digital simulations using the CSMP language. The block diagrams of these programs are shown in Figures 7-a and 7-b respectively; the first of these is a direct simulation of the system,

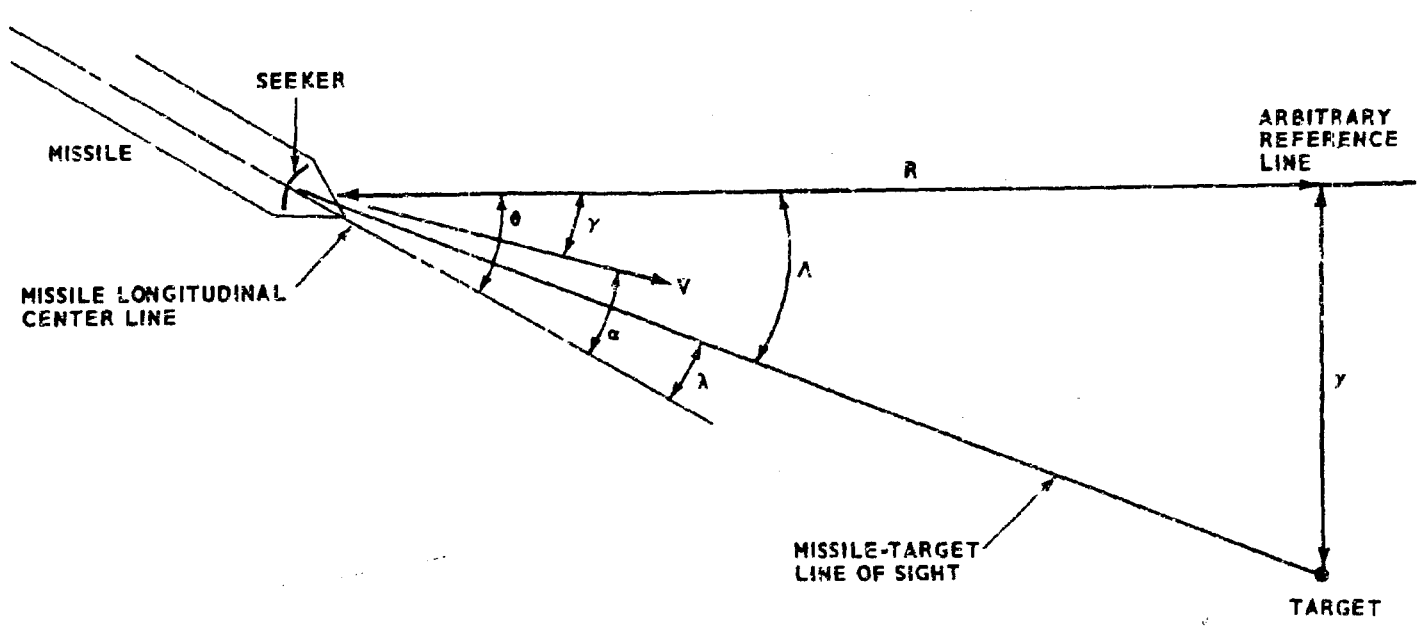

α = MISSILE ANGLE OF ATTACK = θ − γ
θ = MISSILE ATTITUDE WITH RESPECT TO ARBITRARY REFERENCE
γ = MISSILE FLIGHT PATH ANGLE
Λ = MISSILE-TARGET LINE OF SIGHT TO REFERENCE ANGLE
λ = ANGLE BETWEEN MISSILE CENTER LINE AND MISSILE-TARGET LINE OF SIGHT

$\Lambda = \tan^{-1} y/R \simeq y/R$ for $\Lambda \leq 15^{\circ}$

FIGURE 5. SIMPLIFIED HOMING GEOMETRY

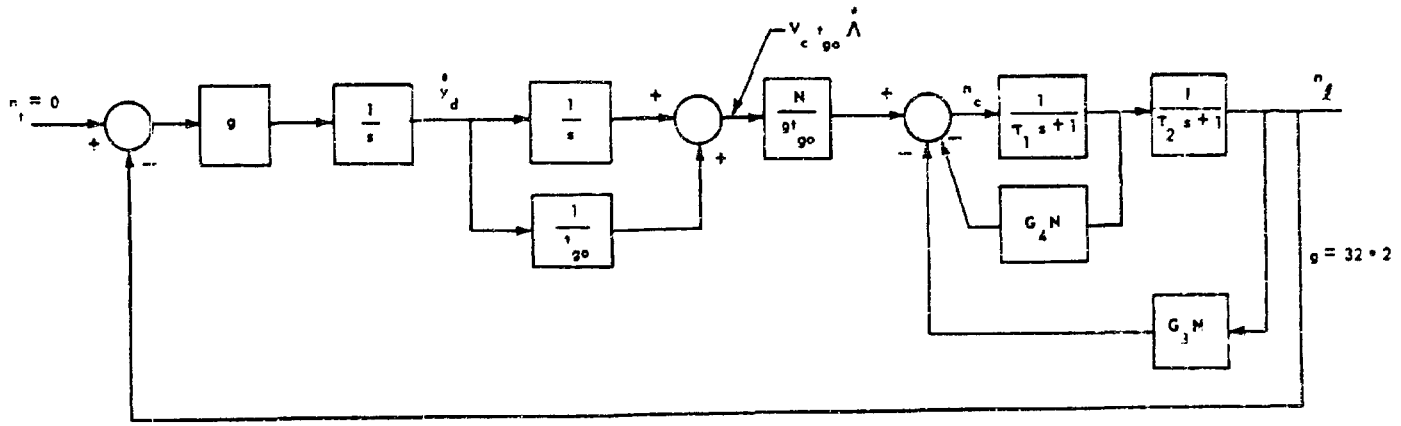

FIGURE 6-a. BLOCK DIAGRAM OF OPTIMUM CONTROLLER

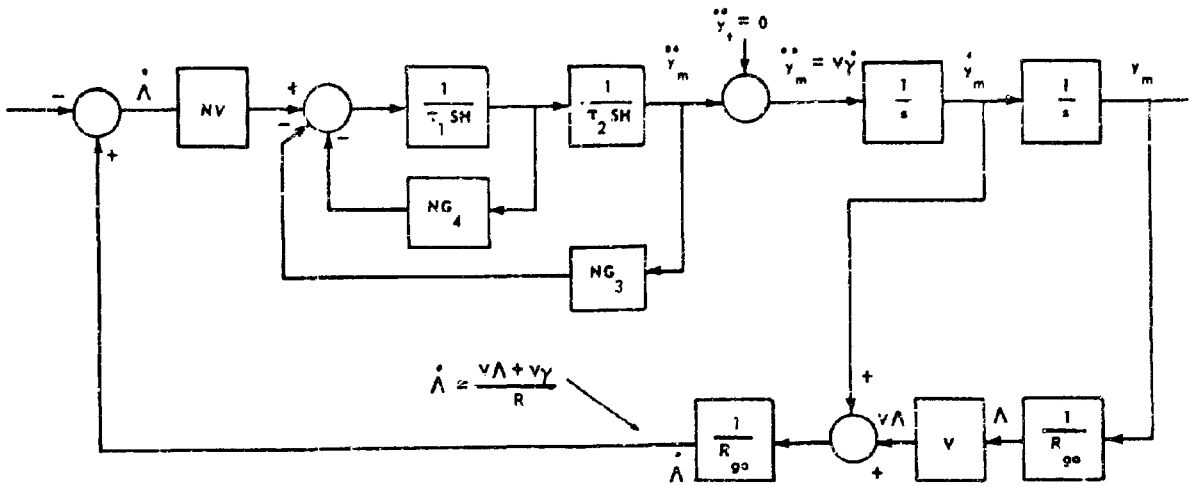

FIGURE 6-b. CONTROLLER MODIFIED WITH $\dot{\Lambda}$ AS INPUT

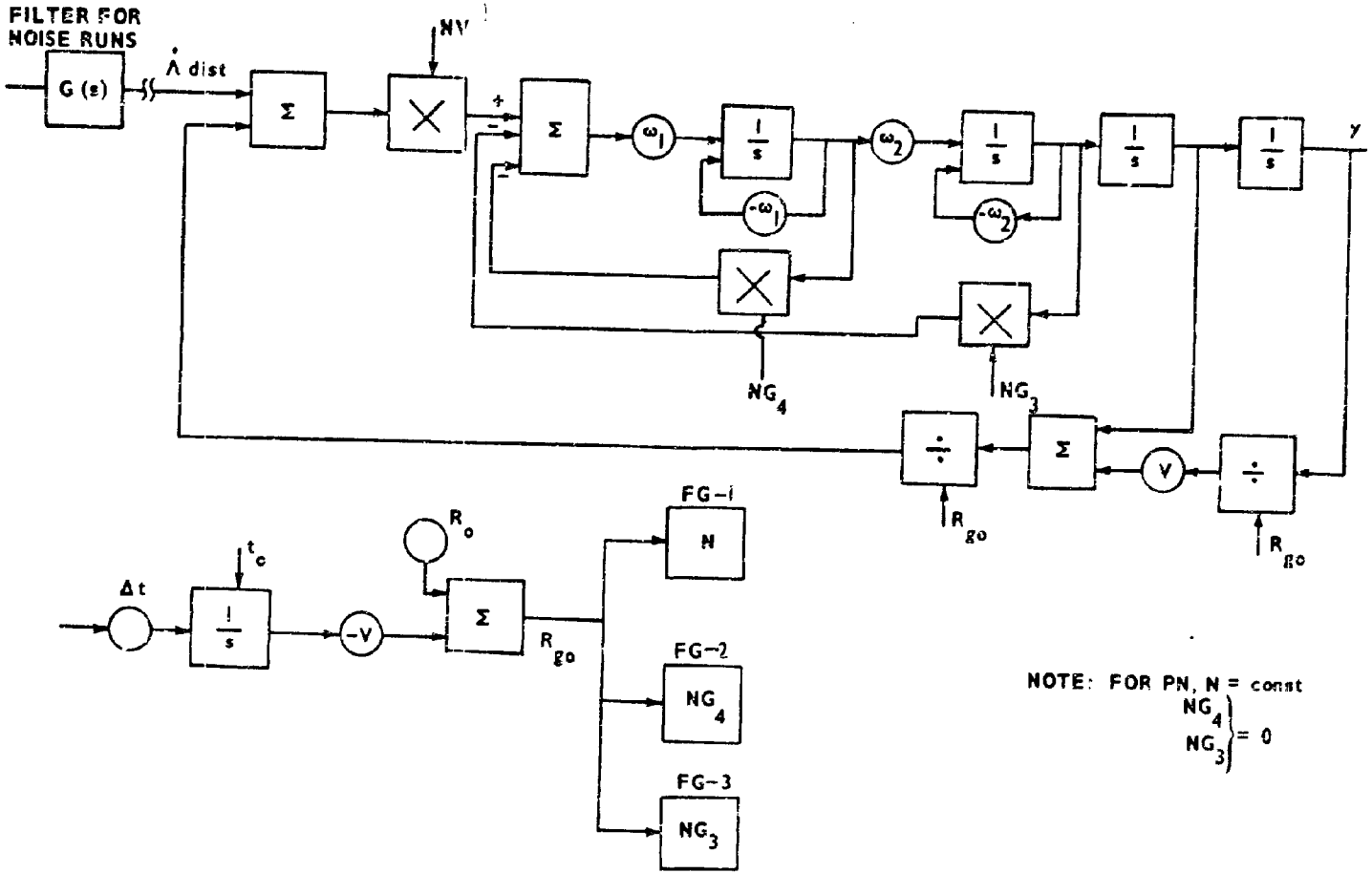

FIGURE 7-a. SIMULATION BLOCK DIAGRAM FOR EXAMPLE SYSTEM

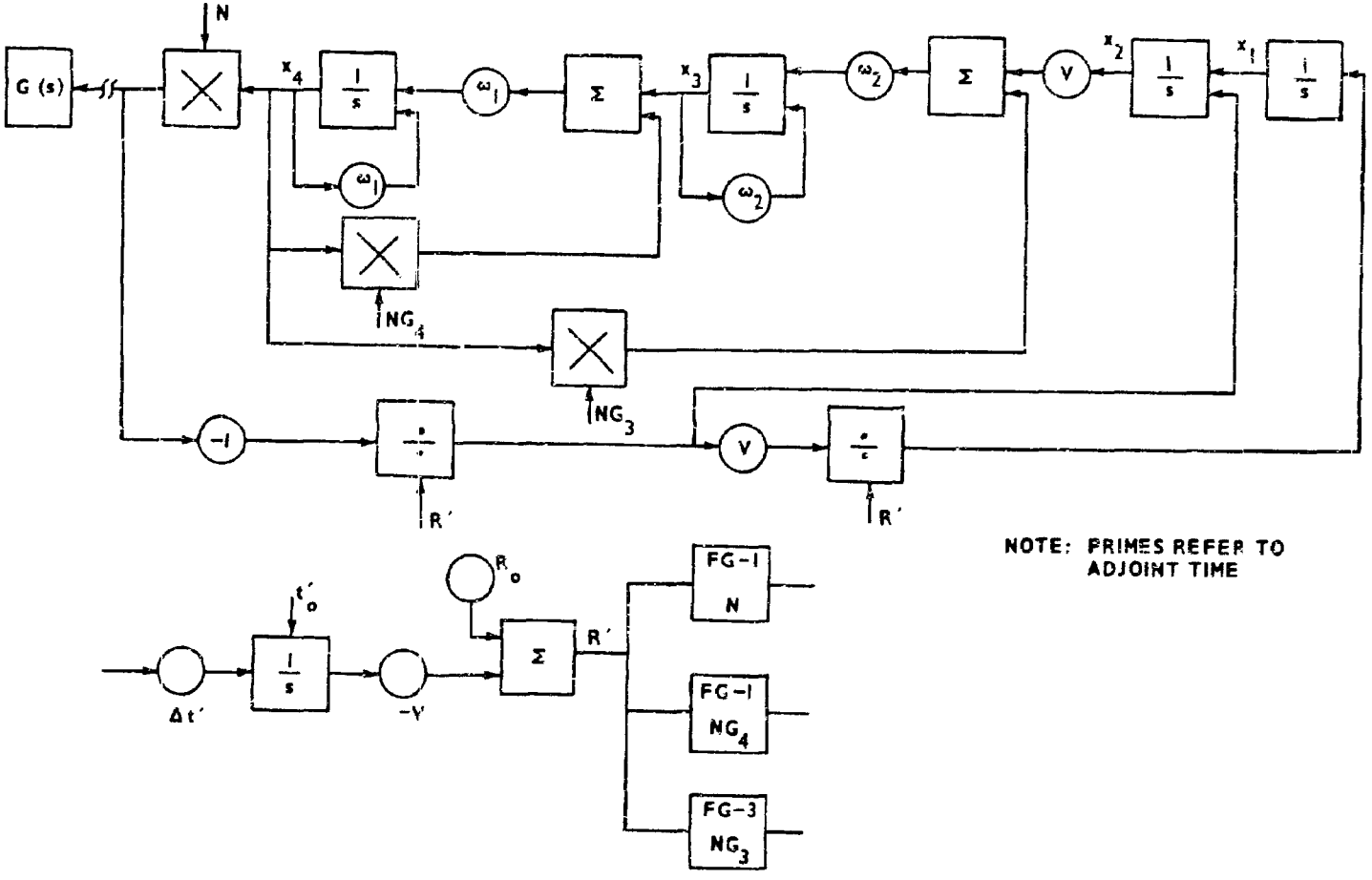

FIGURE 7-b. ADJOINT HOMING MODEL

and the second is an adjoint model used for study of stochastic effects. Each model was used in the PN mode where N was held to a constant, and in the OC mode with time varying coefficients. The specific parameters are summarized in Table I for each case.

TABLE I. SIMULATION PARAMETERS

Parameters	PN	OC
ω_1	1	1
ω_2	2	2
N	4	*
G_3	0	*
G_4	0	*
R_o	10,000 ft	10,000 ft
V	1,000 ft/sec	1,000 ft/sec

*Computed as a function of t_{go} from OC equations.

The complexity of the equations for N, G_3 and G_4 precluded "on line" computation. These values were precomputed, and entered in the simulation as tables. The CSMP function generator takes these tabular values and performs linear interpolation for values of t_{go} lying in between table entries. No effort was made to accurately simulate the subject parameters for very short ranges. Due to mechanization limitations, most seekers have a "blind range" of several hundred feet, and are unable to accurately measure $\dot{\lambda}$. Therefore, N, G_3 and G_4 were linearly decremented to zero, between $t_{go} = 0.5$ and $t_{go} = 0$ sec. These approximate functions are shown in Figures 8-a, 8-b, and 8-c.

The simulation study directly evaluated PN with a gain of 4 to the approximate OC using the parameter approximation described above. A number of input perturbations were considered and the resulting miss distance was measured. Specific disturbances were as follows:

Case I: Impulsive heading disturbance of 1 degree occurring at an arbitrary t_{go}

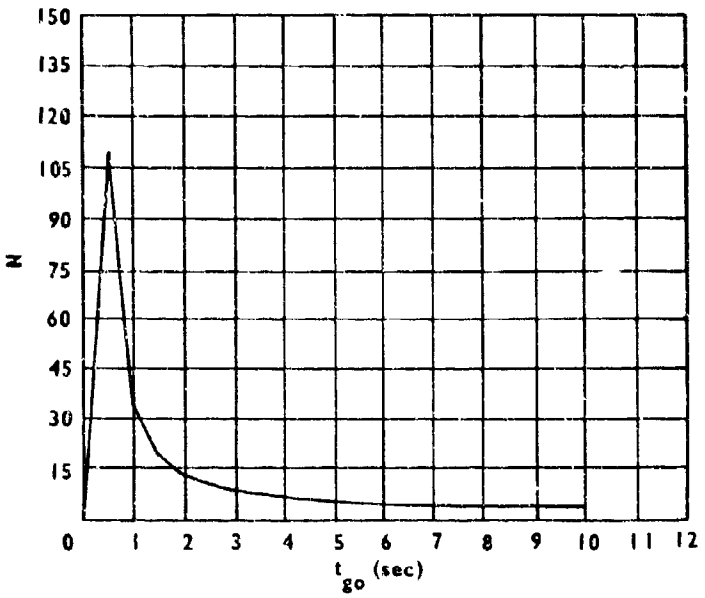

FIGURE 8-a. SIMULATED N FUNCTION

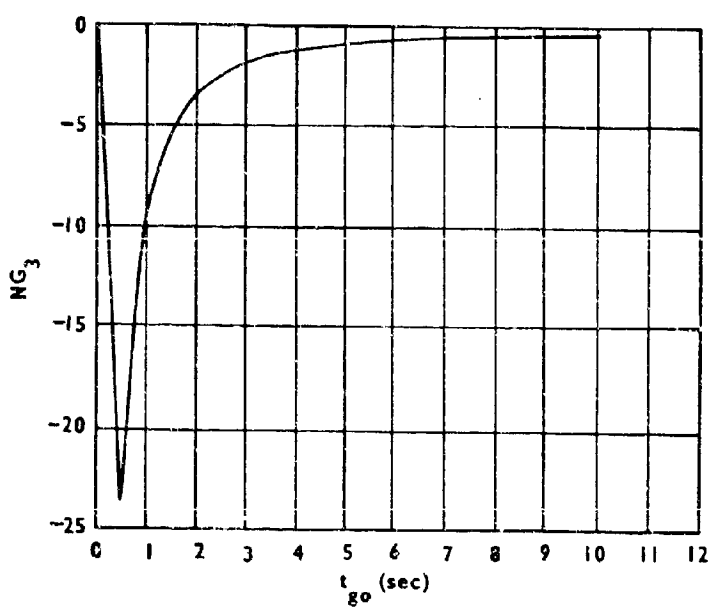

FIGURE 8-b. SIMULATED NG_3 FUNCTION

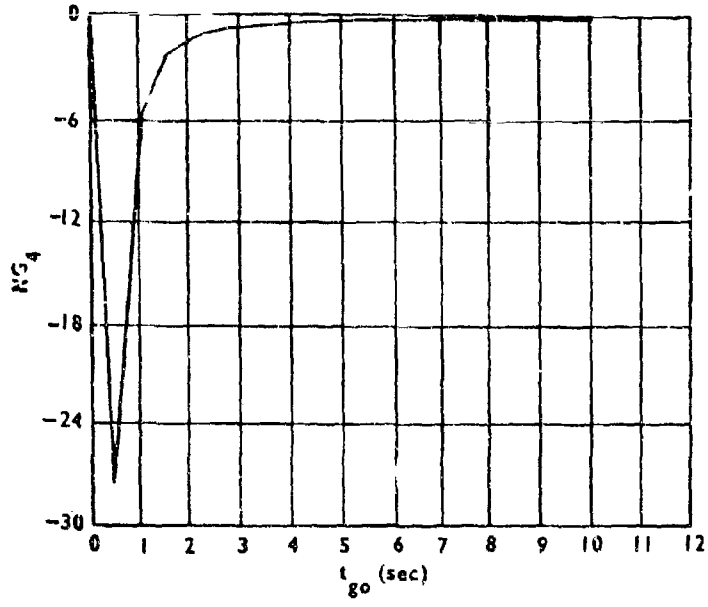

FIGURE 8-c. SIMULATED NG_4 FUNCTION

Case II: Impulsive disturbance on $\dot{\Lambda}$ of $1/6$ degree per second occurring at an arbitrary t_{go}

Case III: Additive wide band noise on $\dot{\Lambda}$ with flat power spectrum in region 0 – 20 hertz

Case IV: Additive narrow band noise on $\dot{\Lambda}$ with a single peaked power spectrum as shown in Figure 9.

The simulation results are shown in Figures 10 through 13, respectively, for each case. It is evident that a dramatic reduction in miss distance results from use of the OC; thus, the added complexity of implementing such a control scheme may in certain instances be well worth the effort.

The OC equations are optimum only if the plant has two time constants. The effect of implementing this OC in a higher order system was also studied. A third time constant of 1 second was added to the plant, and this system was again compared with the use of a constant N. These results are shown in Figures 14 and 15. Evidently the OC is still superior to PN, although performance has degraded somewhat. This is a significant result in that most practical systems are of high order. The above indicates that if an optimum scheme is

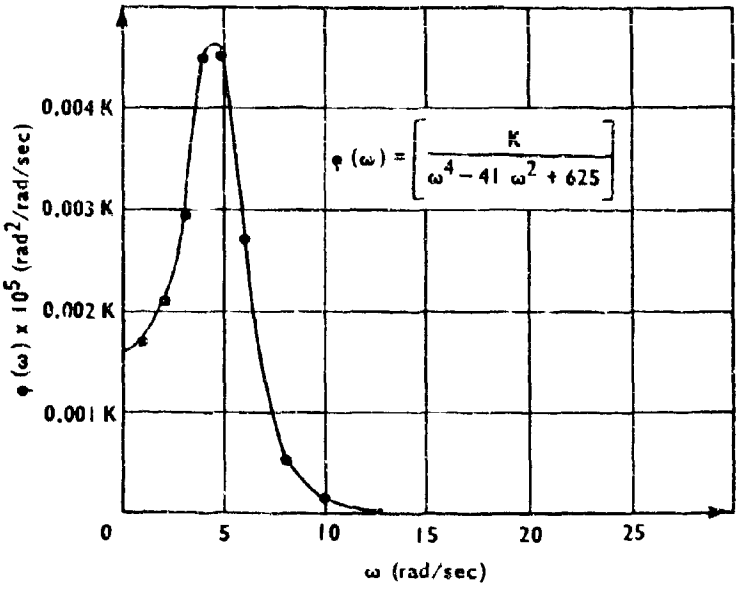

FIGURE 9. NOISE PSD FOR EXAMPLE

derived that accounts for only the predominant time constants (two in this report), the resulting system performance, although suboptimal, would still be superior to PN.

3. The Effective Navigation Ratio

In classical PN the gain N denotes the static ratio of missile turning rate to line-of-sight rate. The gain N is usually a small number between 3 and 5. The plots of N in Appendix B show that for the OC, N takes on very large values relative to the PN case. One is tempted to conclude that the OC requires much higher turn rates than PN. This is not true, however; in Figure 6 it can be seen that the two nonunity feedback terms contribute to the static gain of the loop. The actual value of $\dot{\gamma}/\dot{\Lambda}$ can be computed by reducing the two inner loops and obtaining a single equivalent expression for these. The resulting gain, ignoring missile dynamics, is the navigation ratio for the optimum system. This is given by

$$N_{eff} = \frac{N}{1 + N(G_3 + G_4)} \quad .$$

N_{eff} does not have a large dynamic range. For the numerical example considered herein it hovers in the region

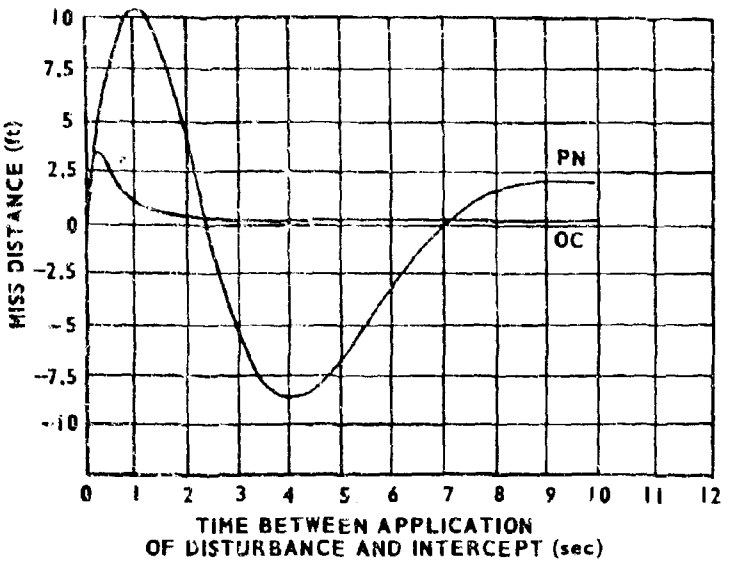

FIGURE 10. MISS DUE TO RANDOM HEADING DISTURBANCES

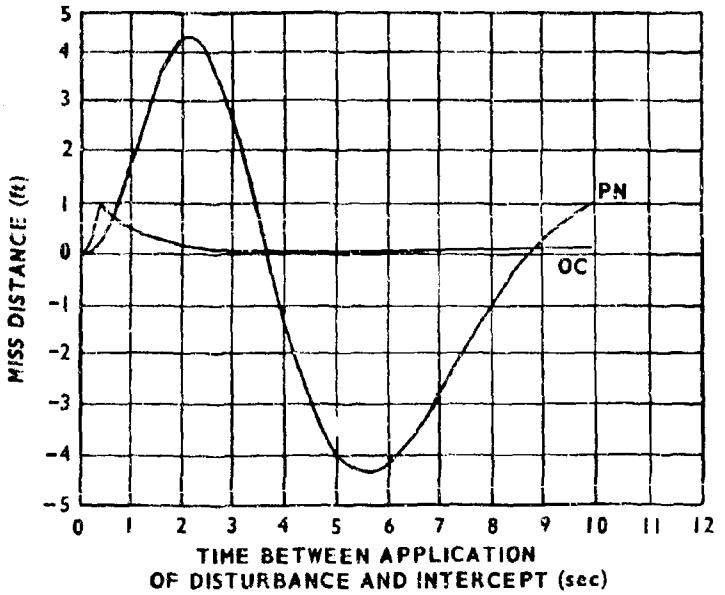

FIGURE 11. MISS DUE TO RANDOM DISTURBANCE ON $\dot{\lambda}$

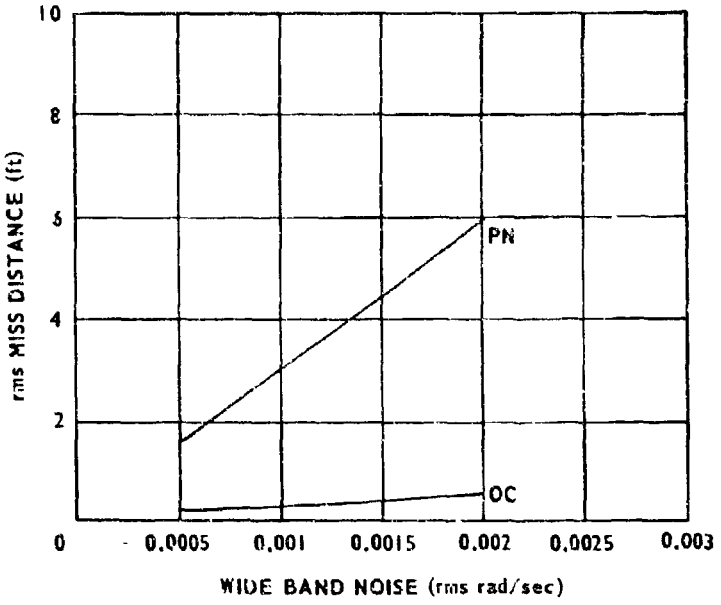

FIGURE 12. SYSTEM RESPONSE TO WIDE BAND NOISE

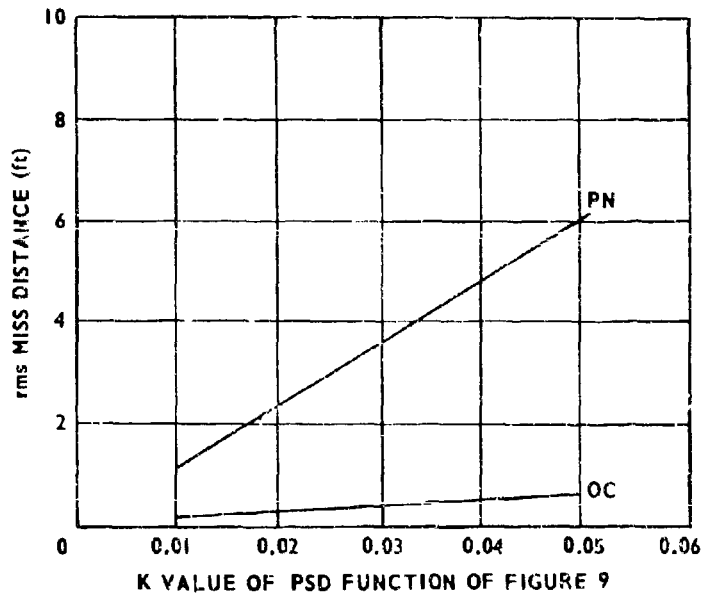

FIGURE 13. MISS DUE TO NARROW BAND NOISE

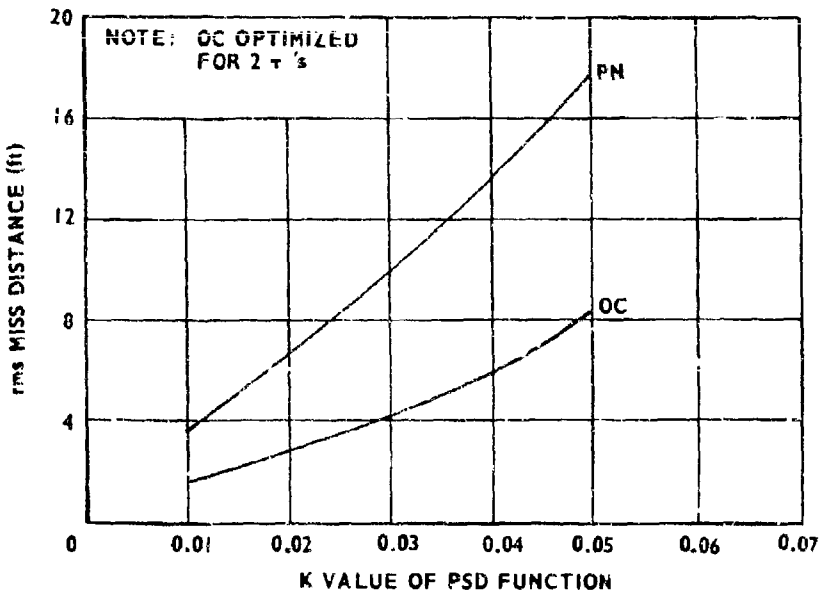

FIGURE 14. MISS DUE TO NARROW BAND NOISE FOR THREE-TIME CONSTANT SYSTEM

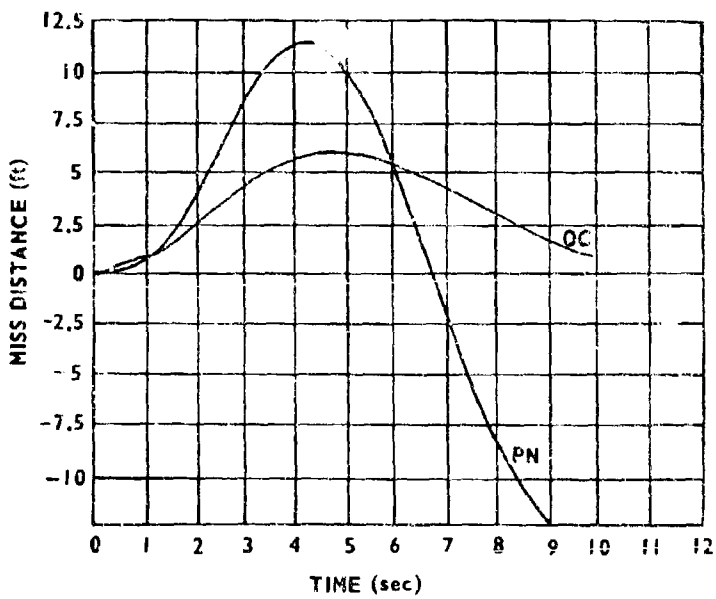

FIGURE 15. MISS DUE TO RANDOM DISTURBANCE ON $\dot{\lambda}$ (SYSTEM WITH THREE τ's)

$$2 < N < 3;$$

thus, the OC does not require increased missile performance.

4. The Effect of the Parameter λ

The quantity λ represents a weight on the parameter N. For large values of t_{go} it has little or no effect, but reduces N heavily when t_{go} is small. This effect can be seen in Appendix B, if one compares the plots of N for λ = 0 with those for λ = 1. Since λ reduces N near intercept, it obviously reduces required missile maneuver, since N_{eff} is also reduced in magnitude. Since λ is thus a significant design parameter, how does one choose a "good" value? This problem is intimately tied to each specific missile design, since it relates directly to available maneuver capability. From Figure 6-a, the called-for maneuver in G can be written

$$n_c = \frac{V_c \dot{\Lambda}}{g} \left[\frac{N}{1 + N(G_3 + G_4)} \right] = \frac{V_c \dot{\Lambda}}{g} N_{eff} \quad .$$

By defining the maximum available maneuver as n_{max}, the following expression can be derived from the above equation:

$$N_{eff} = \frac{n_{max} g}{V_c \dot{\Lambda}} \quad .$$

The terms on the right side of this equation can be established for a given missile and engagement configuration. Thus, the maximum practical value of N_{eff} is defined, and this in turn infers a specific λ, since there is no need in generating values of N_{eff} that result in a called-for missile maneuver in excess of performance limits. The penalty, of course, is that for λ > 0, the miss distance will increase over that obtainable with λ = 0. This is illustrated in Figure 16 for the example system.

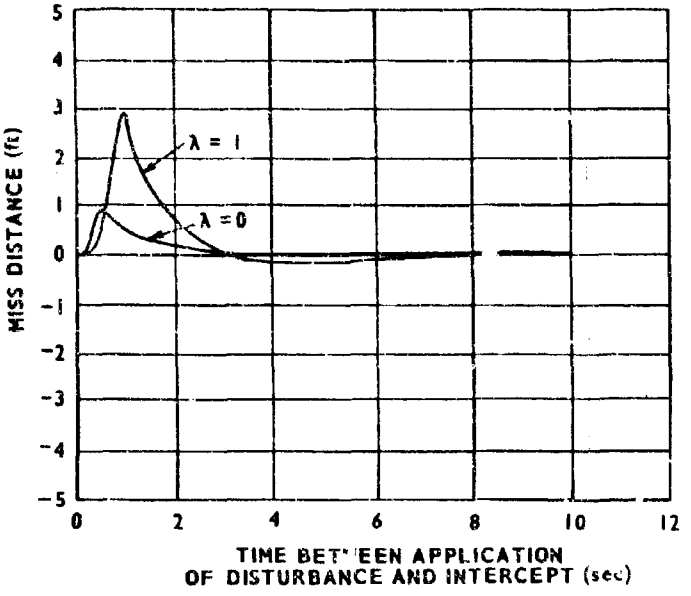

FIGURE 16. EFFECT OF VARYING λ ON MISS DUE TO RANDOM DISTURBANCE ON $\dot{A}$

Section V. MECHANIZATION CONSIDERATIONS

A mathematically elegant solution is useless if hardware implementation is not practical. As mentioned before, N, G_3 and G_4 can be generated by analog (diode function generators) or digital (read-only memories) means. The input to such devices would be t_{go}, thus requiring a measurement of this quantity. For stationary or slow-moving targets, t_{go} can be estimated closely by knowledge of the initial range and missile velocity profile. Intercept of fast targets that contribute considerably to the closing velocity is more difficult, since ranging must be obtained during flight. This requires tracking of both interceptor and target by either ground radar or an active ranging device on board the interceptor.

Another major consideration is that the OC requires that all system states be measured. The actual missile acceleration can be measured with an accelerometer; y_d and $\dot{y}_d$ are implicitly measured by the seeker as previously shown. The remaining state (x_4 in Figure 4) cannot be measured if the two time constants are assumed to represent the airframe. However, if in an n^{th} order system (n-1) states are measurable, the n^{th} one can be estimated by "observer pole" techniques [6-8]. Finally, if the target acceleration term G_5 is to be included, $\ddot{y}_t$ must also be measured. This requirement, although difficult to meet, is no different from the requirement for implementation of biased PN, where a bias term is appended in order to reduce the miss caused by target evasion.

Certain types of missiles are required to operate through a wide altitude band, where air density considerably affects the airframe time constants; for such missiles, ω_1 and ω_2 cannot be assumed constant. This problem also exists in conventional systems required to operate in such an environment. The solution is to generate a family of functions N, G_3 and G_4, each valid for a specific altitude band. The controller would then be "band-switched" to the appropriate functions, dependent on the altitude.

The values of N shown in Appendix B are plotted in log-log coordinate paper. It is seen that for the vast majority of cases, N can be approximated by a few straight line segments in the log-log plane. This suggests a very simple mechanization scheme for N. The above linear relationship implies that

$$\ell n\ N = C_i + b_i\ \ell n\ t_{go} \Big|_{\text{region i}},$$

where C_i is a suitable intercept and b_i is the signed slope of the straight line approximation.

A family of equations as above can be mechanized as shown in Figure 17.

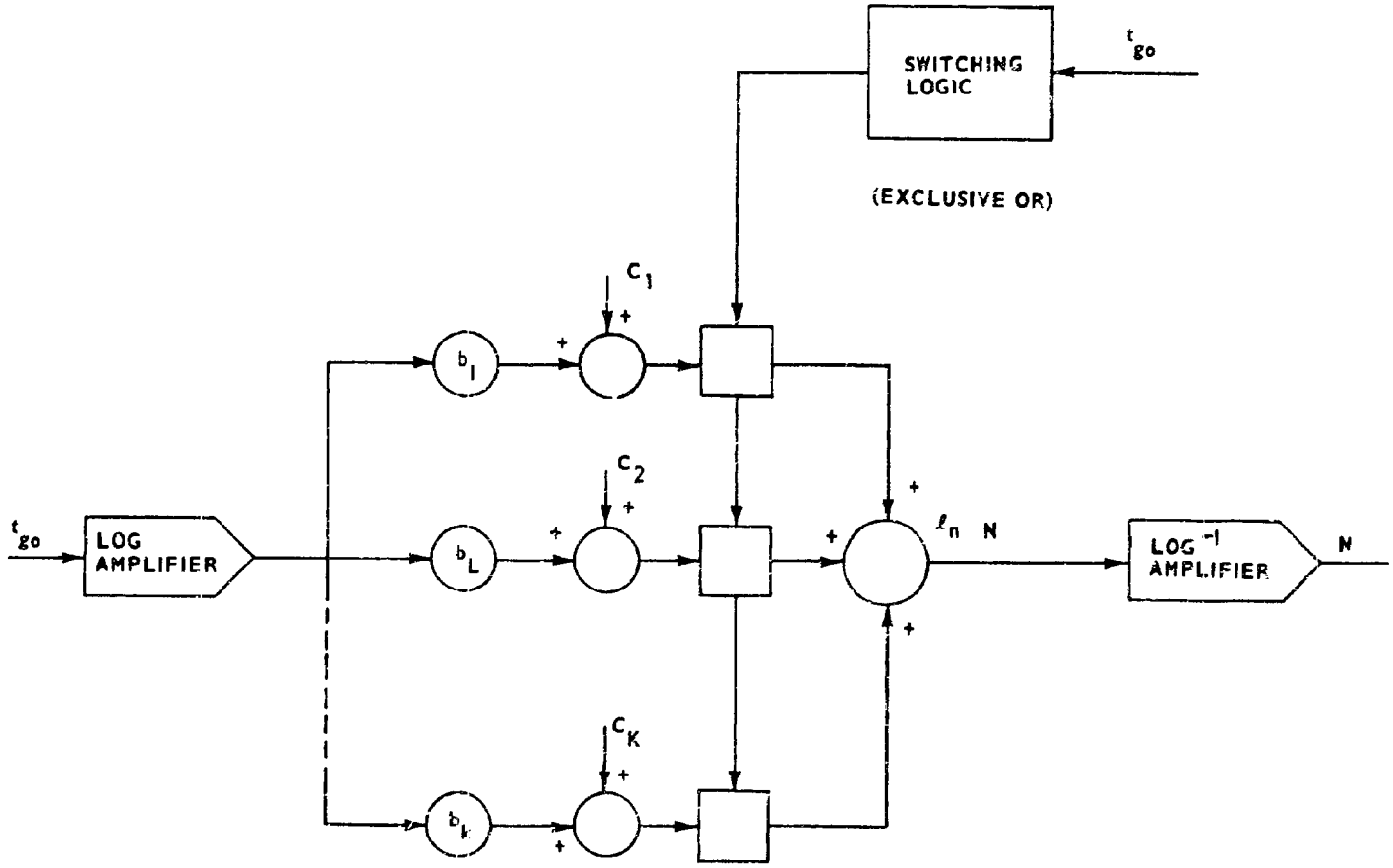

FIGURE 17. FEASIBLE CONCEPT FOR APPROXIMATING N

Section VI. CONCLUSIONS

The problem solved herein is an extension of the work begun in 1968 [4]. The basic homing system has been augmented by two time constants and cast as a minimum regulator problem. Simulation using the resulting controller equations indicates that the optimal approach results in a guidance scheme superior to PN.

Practical problems have been considered and it is concluded that the OC concept is feasible from a mechanization viewpoint. The added complexity must be weighed against the substantial payoff in drastically reduced miss distances.

The behavior of the OC derived herein is consistent with previously derived results. For very large t_{go}, N is assymptotic to 3. As the time constants approach 0 ($\omega_i \rightarrow \infty$) N approaches 3 and G_3 and G_4 approach 0. Thus for very large t_{go} or very small time constants, the OC approaches classical PN with a gain N = 3.

Appendix A
COMPUTATION OF COMPONENT TERMS OF F(t)

$$F(T-t) = F\left(t_{go}\right) = F(t)_{t = t_{go}}$$

$$a_{11} = \mathcal{L}^{-1}\left[\frac{1}{s} - \frac{g^2\,\omega_1^2\,\omega_2^2}{\lambda}\left(\frac{1}{s^4(s+\omega_1)(s-\omega_1)(s+\omega_2)(s-\omega_2)}\right)\right]$$

$$= \mathcal{L}^{-1}\left[\frac{1}{s} - \frac{g^2}{\lambda}\left(\frac{1}{s^4} + \frac{\frac{\omega_1^2+\omega_2^2}{\omega_1^2\,\omega_2^2}}{s^2} - \frac{\frac{\omega_2^2}{2\omega_1^3(\omega_1^2-\omega_2^2)}}{s+\omega_1} + \frac{\frac{\omega_2^2}{2\omega_1^3(\omega_1^2-\omega_2^2)}}{s-\omega_1}\right.\right.$$

$$\left.\left. + \frac{\frac{\omega_1^2}{2\omega_2^3(\omega_1^2-\omega_2^2)}}{s+\omega_2} - \frac{\frac{\omega_1^2}{2\omega_2^3(\omega_1^2-\omega_2^2)}}{s-\omega_2}\right)\right]$$

$$a_{11} = 1 - \frac{g^2}{\lambda}\left[\frac{t^3}{3} + \left(\frac{\omega_1^2+\omega_2^2}{\omega_1^2\omega_2^2}\right)t + \frac{\omega_2^2}{2\omega_1^3(\omega_1^2-\omega_2^2)}\left(e^{\omega_1 t} - e^{-\omega_1 t}\right) + \frac{\omega_1^2}{2\omega_2^3(\omega_1^2-\omega_2^2)}\left(e^{-\omega_2 t} - e^{\omega_2 t}\right)\right]$$

$$a_{21} = \mathcal{L}^{-1}\left[\frac{g^2\,\omega_1^2\,\omega_2^2}{\lambda}\left(\frac{1}{s^3(s+\omega_1)(s-\omega_1)(s+\omega_2)(s-\omega_2)}\right)\right]$$

$$= \mathcal{L}^{-1}\left\{\frac{g^2\omega_1^2\omega_2^2}{\lambda}\left[\frac{\frac{1}{\omega_1^2\omega_2^2}}{s^3} + \frac{\frac{\omega_1^2+\omega_2^2}{\omega_1^4\omega_2^4}}{s} + \frac{1}{2\omega_1^4(\omega_1^2-\omega_2^2)}\left(\frac{1}{s+\omega_1} + \frac{1}{s-\omega_1}\right)\right.\right.$$

$$\left.\left. - \frac{1}{2\omega_2^4(\omega_1^2-\omega_2^2)}\left(\frac{1}{s+\omega_2} + \frac{1}{s-\omega_2}\right)\right]\right\}$$

$$a_{21} = \frac{g^2}{\lambda}\left[\frac{t^2}{2} + \frac{\omega_1^2+\omega_2^2}{\omega_1^2\,\omega_2^2} + \frac{\omega_2^2}{2\omega_1^2(\omega_1^2-\omega_2^2)}\left(e^{-\omega_1 t} + e^{\omega_1 t}\right) - \frac{\omega_1^2}{2\omega_2^2(\omega_1^2-\omega_2^2)}\left(e^{-\omega_2 t} + e^{\omega_2 t}\right)\right]$$

$$a_{31} = \mathcal{L}^{-1}\left[\frac{g\,\omega_1^2\omega_2^2}{\lambda}\left(\frac{1}{s^2(s+\omega_1)(s-\omega_1)(s+\omega_2)(s-\omega_2)}\right)\right]$$

$$= \mathcal{L}^{-1}\left\{\frac{g\,\omega_1^2\omega_2^2}{\lambda}\left[\frac{1}{\omega_1^2\omega_2^2 s^2} + \frac{1}{2\omega_1^3(\omega_1^2-\omega_2^2)}\left(\frac{1}{s-\omega_1} - \frac{1}{s+\omega_1}\right)\right.\right.$$

$$\left.\left. + \frac{1}{2\omega_2^3(\omega_1^2-\omega_2^2)}\left(\frac{1}{s+\omega_2} - \frac{1}{s-\omega_2}\right)\right]\right\}$$

$$a_{31} = \frac{g}{\lambda}\left[t + \frac{\omega_2^2}{2\omega_1(\omega_1^2-\omega_2^2)}\left(e^{\omega_1 t} - e^{-\omega_1 t}\right) + \frac{\omega_1^2}{2\omega_2(\omega_1^2-\omega_2^2)}\left(e^{-\omega_2 t} - \quad\right)\right]$$

$$a_{41} = \mathcal{L}^{-1}\left[\frac{-g\,\omega_1^2\omega_2}{\lambda}\left(\frac{1}{s^2(s-\omega_1)(s+\omega_1)(s+\omega_2)}\right)\right]$$

$$= \mathcal{L}^{-1}\left[-\frac{1}{\omega_1^2\omega_2 s^2} + \frac{1}{\omega_1^2\omega_2^2 s} + \frac{1}{2\omega_1^3(\omega_1+\omega_2)}\left(\frac{1}{s-\omega_1}\right) + \frac{1}{2\omega_1^3(\omega_1-\omega_2)}\left(\frac{1}{s+\omega_1}\right)\right.$$

$$\left. - \frac{1}{\omega_2^2(\omega_1^2-\omega_2^2)}\left(\frac{1}{s+\omega_2}\right)\right]$$

$$a_{41} = -\frac{g}{\lambda}\left[-t + \frac{1}{\omega_2} + \frac{\omega_2}{2\omega_1(\omega_1+\omega_2)}\,e^{\omega_1 t} + \frac{\omega_2}{2\omega_1(\omega_1-\omega_2)}\,e^{-\omega_1 t} - \frac{\omega_1^2\,e^{-\omega_2 t}}{\omega_2(\omega_1^2-\omega_2^2)}\right]$$

$$a_{12} = \mathcal{L}^{-1}\left(-\frac{1}{s^2}\right)$$

$$a_{12} = -t$$

$$a_{22} = \mathcal{L}^{-1}\left(\frac{1}{s}\right)$$

$$a_{22} = u(t) = 1 \text{ in solution interval}$$

$$a_{13} = \mathcal{L}^{-1}\left(\frac{-g}{s^2(s-\omega_2)}\right)$$

$$a_{13} = \mathcal{L}^{-1}\left(-\frac{\frac{1}{\omega_2}}{s^2} - \frac{\frac{1}{\omega_2^2}}{s} + \frac{\frac{1}{\omega_2^2}}{s-\omega_2} \right)$$

$$a_{13} = g\left(\frac{t}{\omega_2} + \frac{1}{\omega_2^2} - \frac{e^{\omega_2 t}}{\omega_2^2} \right)$$

$$a_{23} = \mathcal{L}^{-1}\left(\frac{g}{s\,(s-\omega_2)} \right)$$

$$a_{23} = -\,g\left(\frac{1}{\omega_2} - \frac{e^{\omega_2 t}}{\omega_2} \right)$$

$$a_{33} = \mathcal{L}^{-1}\left(\frac{1}{s-\omega_2} \right) = e^{\omega_2 t}$$

$$a_{14} = \mathcal{L}^{-1}\left(\frac{g\,\omega_2}{s^2\,(s-\omega_1)\,(s-\omega_2)} \right)$$

$$= \mathcal{L}^{-1}\left\{ g\,\omega_2 \left[\frac{\frac{1}{\omega_1\omega_2}}{s^2} + \frac{\frac{\omega_1+\omega_2}{\omega_1^2\omega_2^2}}{s} + \frac{\frac{1}{\omega_1^2\,(\omega_1-\omega_2)}}{(s-\omega_1)} - \frac{\frac{1}{\omega_2^2\,(\omega_1-\omega_2)}}{(s-\omega_2)} \right] \right\}$$

$$a_{14} = g\,\omega_2 \left(\frac{1}{\omega_1\omega_2}\,t + \frac{\omega_1+\omega_2}{\omega_1^2\omega_1^2} + \frac{1}{\omega_1^2\,(\omega_1-\omega_2)}\,e^{\omega_1 t} - \frac{1}{\omega_2^2\,(\omega_1-\omega_2)}\,e^{\omega_2 t} \right)$$

$$a_{24} = \mathcal{L}^{-1}\left(\frac{-\,g\,\omega_2}{s\,(s-\omega_1)\,(s-\omega_2)} \right)$$

$$= \mathcal{L}^{-1}\left\{ -\,g\,\omega_2 \left[\frac{\frac{1}{\omega_1\omega_2}}{s} + \frac{\frac{1}{\omega_1(\omega_1-\omega_2)}}{(s-\omega_1)} - \frac{\frac{1}{\omega_2\,(\omega_1-\omega_2)}}{s-\omega_2} \right] \right\}$$

$$a_{24} = -\,g\,\omega_2 \left[\frac{1}{\omega_1\omega_2} + \frac{1}{\omega_1\,(\omega_1-\omega_2)}\,e^{\omega_1 t} - \frac{1}{\omega_2\,(\omega_1-\omega_2)}\,e^{\omega_2 t} \right]$$

$$a_{34} = \mathcal{L}^{-1}\left(\frac{-\,\omega_2}{(s-\omega_1)\,(s-\omega_2)} \right)$$

$$a_{34} = -\frac{\omega_2}{\omega_1-\omega_2}\left(e^{\omega_1 t} - e^{\omega_2 t}\right)$$

$$a_{44} = \mathcal{L}^{-1}\left(\frac{1}{s-\omega_1}\right) = e^{\omega_1 t}$$

$$k = \mathcal{L}^{-1}\left(\frac{-g\,\omega_2}{s^2\,(s+\omega_1)\,(s+\omega_2)}\right)$$

By analogy to a_{14} k is given by:

$$k = -g\,\omega_2\left(\frac{1}{\omega_1\omega_2}t - \frac{\omega_1+\omega_2}{\omega_1^2\omega_2^2} + \frac{1}{\omega_1^2\,(\omega_1-\omega_2)}e^{-\omega_1 t} + \frac{1}{\omega_2^2\,(\omega_1-\omega_2)}e^{-\omega_2 t}\right)$$

Appendix B
NUMERICAL DATA FOR OPTIMUM CONTROLLER GAINS

The numerical values for the functions N, G_3 and G_4 were computed via digital program for a wide range of values of ω_1 and ω_2. The data are presented in this appendix in the form of plots of the subject functions versus t_{go} (Figures B-1 through B-19). The time span considered is 10 seconds, which should cover most practical applications. The assymptotic nature of the functions allows easy extrapolation from the plots if somewhat longer time spans are deemed desirable. In some instances, particularly where $\omega_1 = \omega_2$, the computation of N involves differences of large, almost equal numbers; for this reason, double precision arithmetic was found necessary.

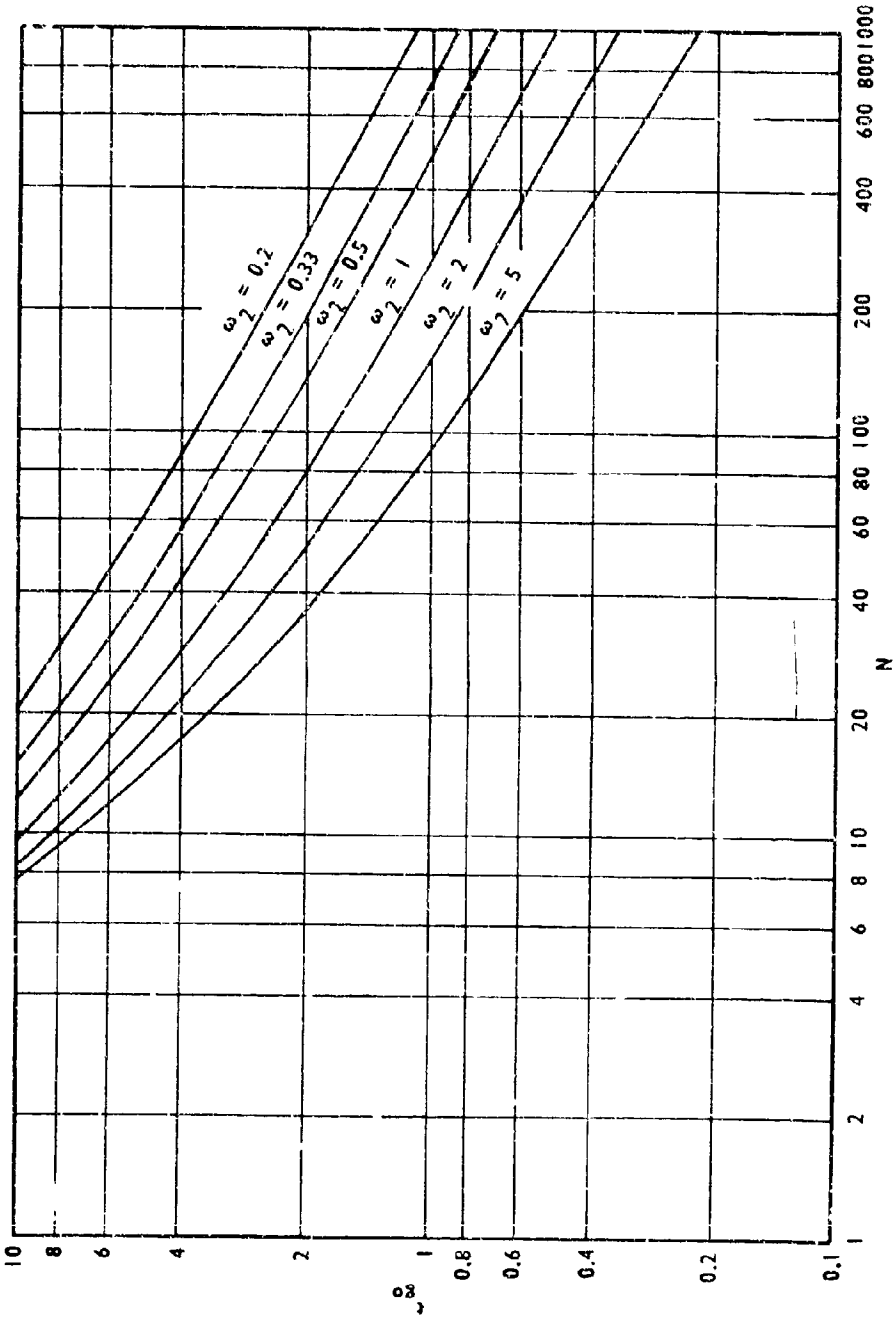

FIGURE B-1. N VERSUS t_{go} FOR $\omega_1 = 0.2$, $\lambda = 0$

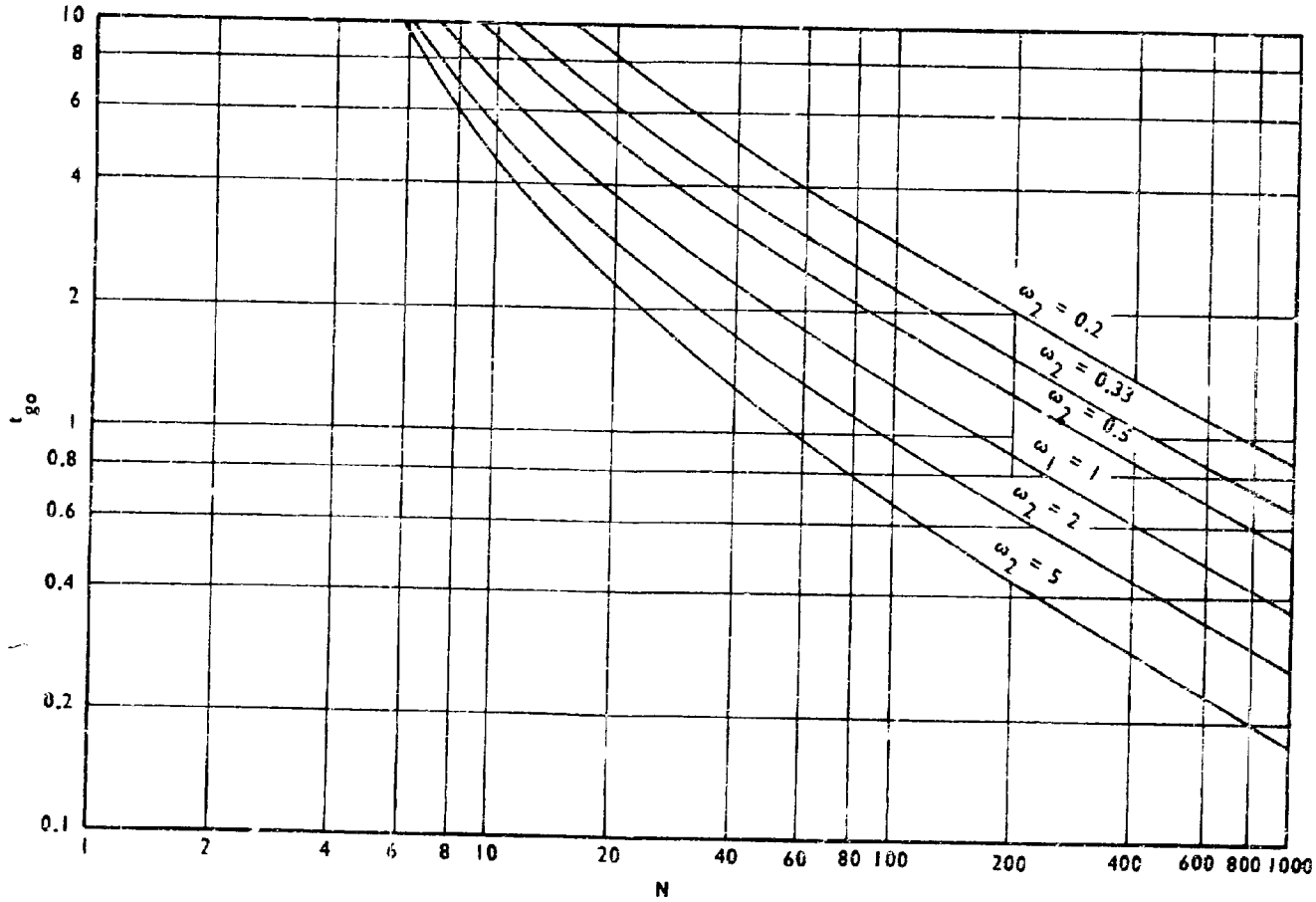

FIGURE B-2. N VERSUS t_{go} FOR $\omega_1 = 0.33$, $\lambda = 0$

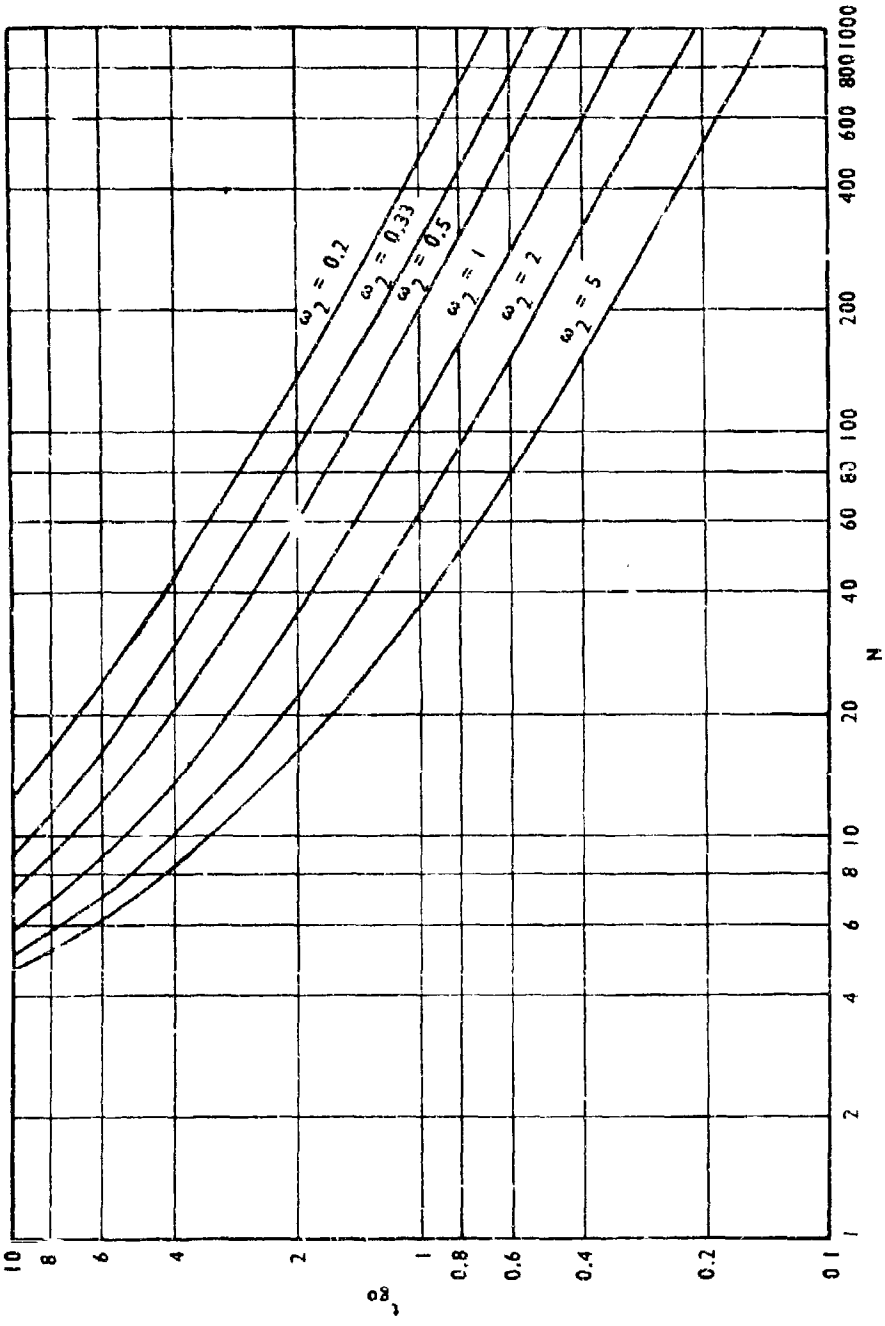

FIGURE B-3. N VERSUS t_{go} FOR $\omega_1 = 0.5$, $\lambda = 0$

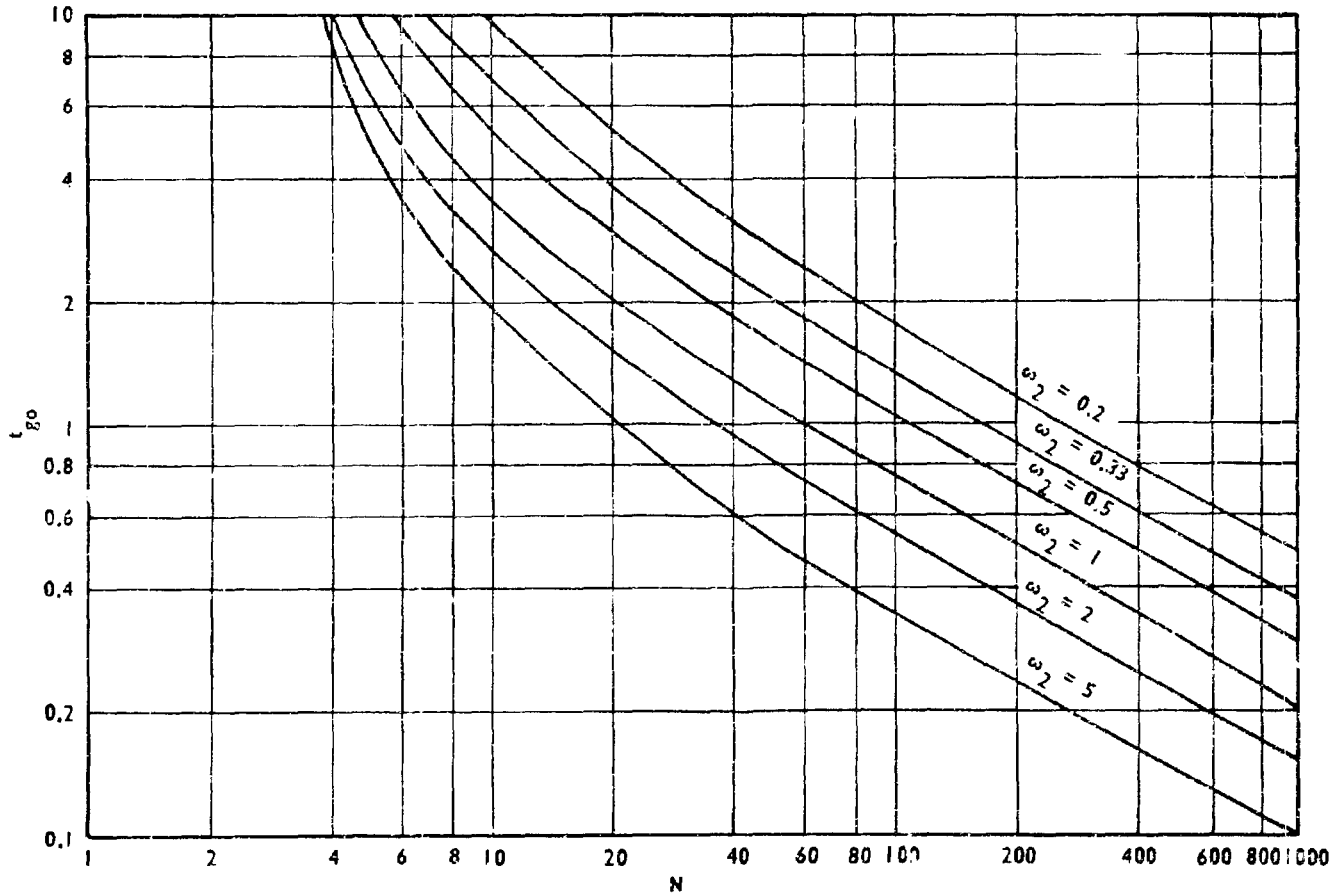

FIGURE B-4. N VERSUS t_{go} FOR $\omega_1 = 1$, $\lambda = 0$

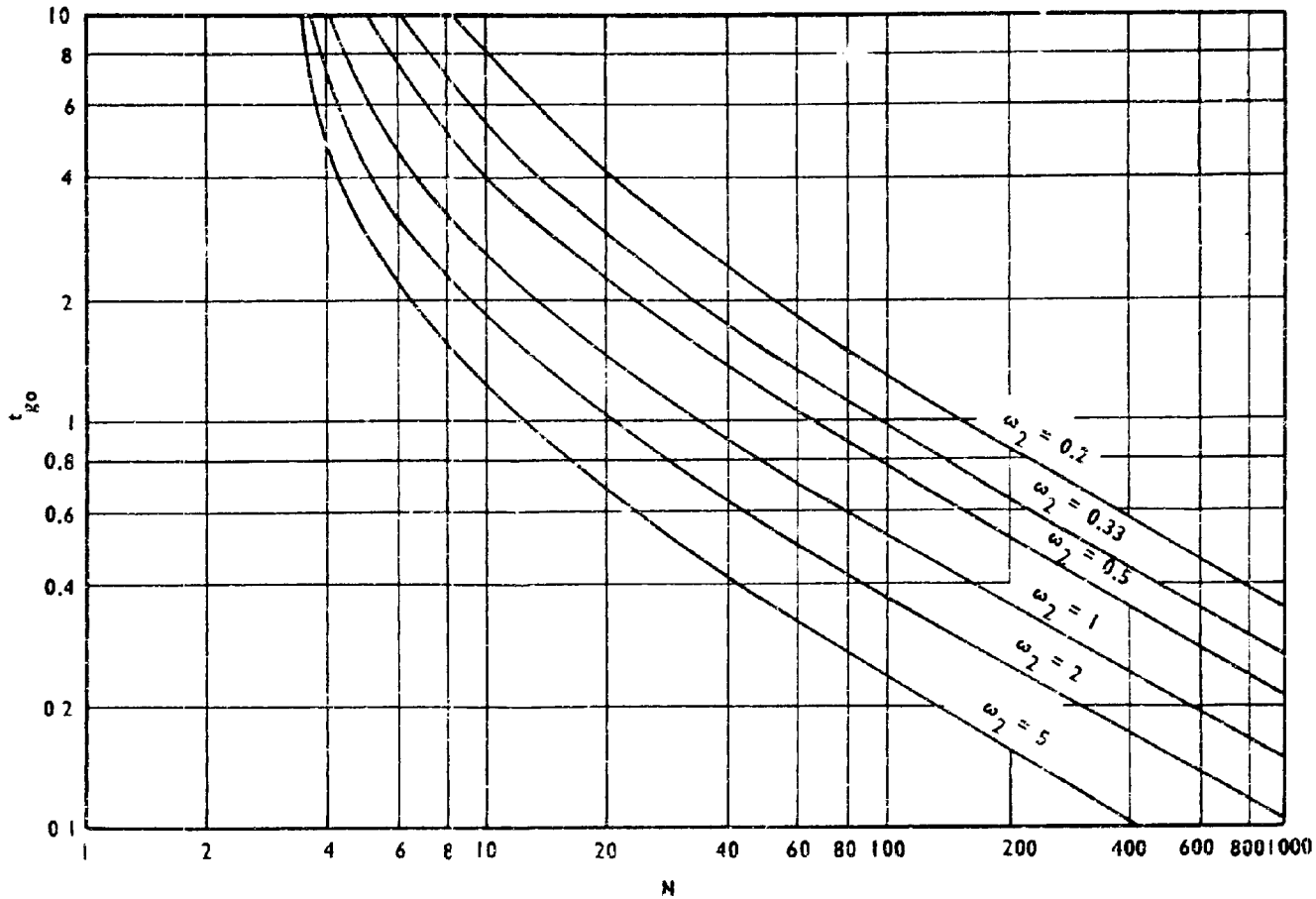

FIGURE B-5. N VERSUS t_{go} FOR $\omega_1 = 2$, $\lambda = 0$

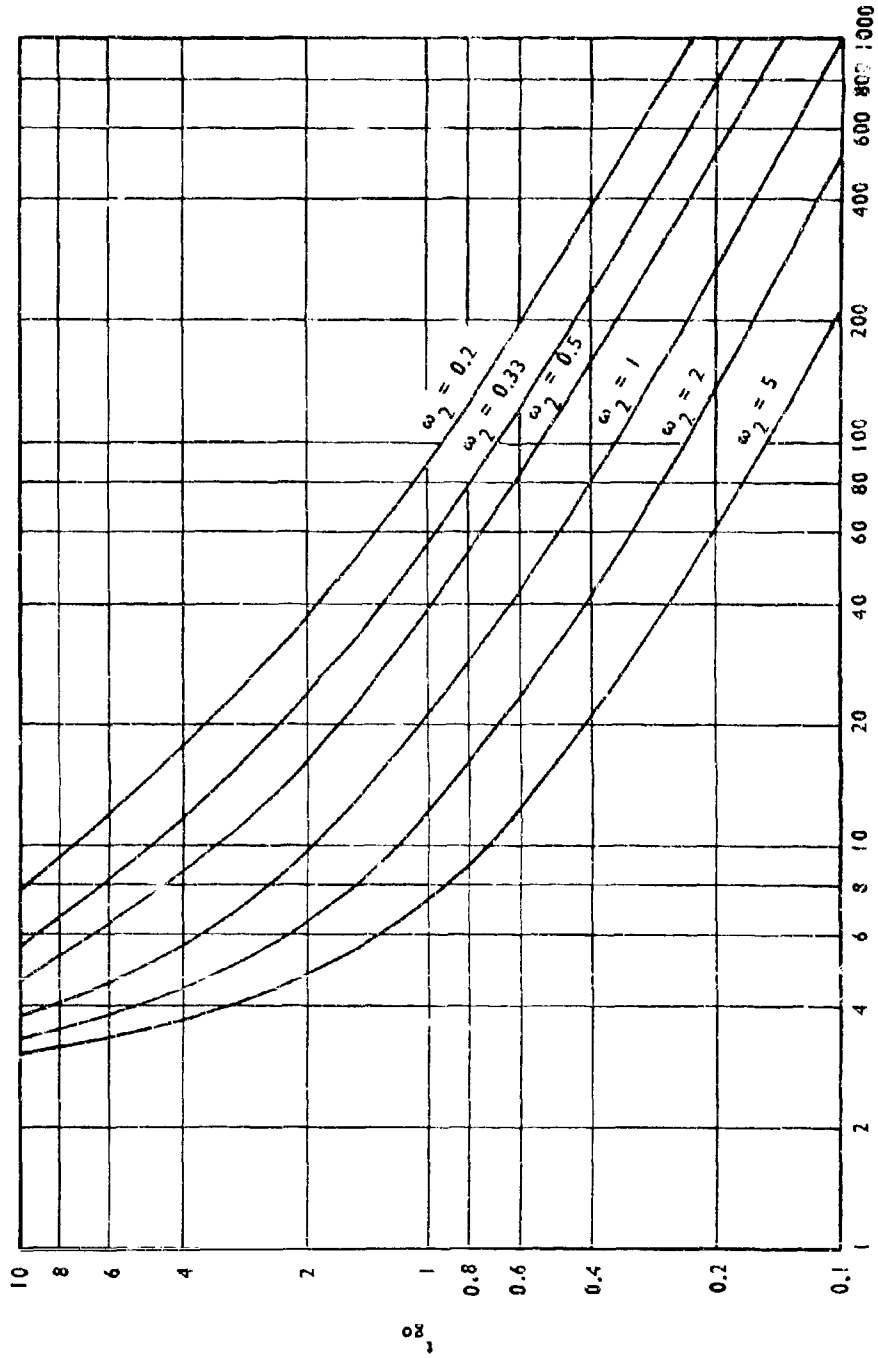

FIGURE B-6. N VERSUS t_{go} FOR $\omega_1 = 5$, $\lambda = 0$

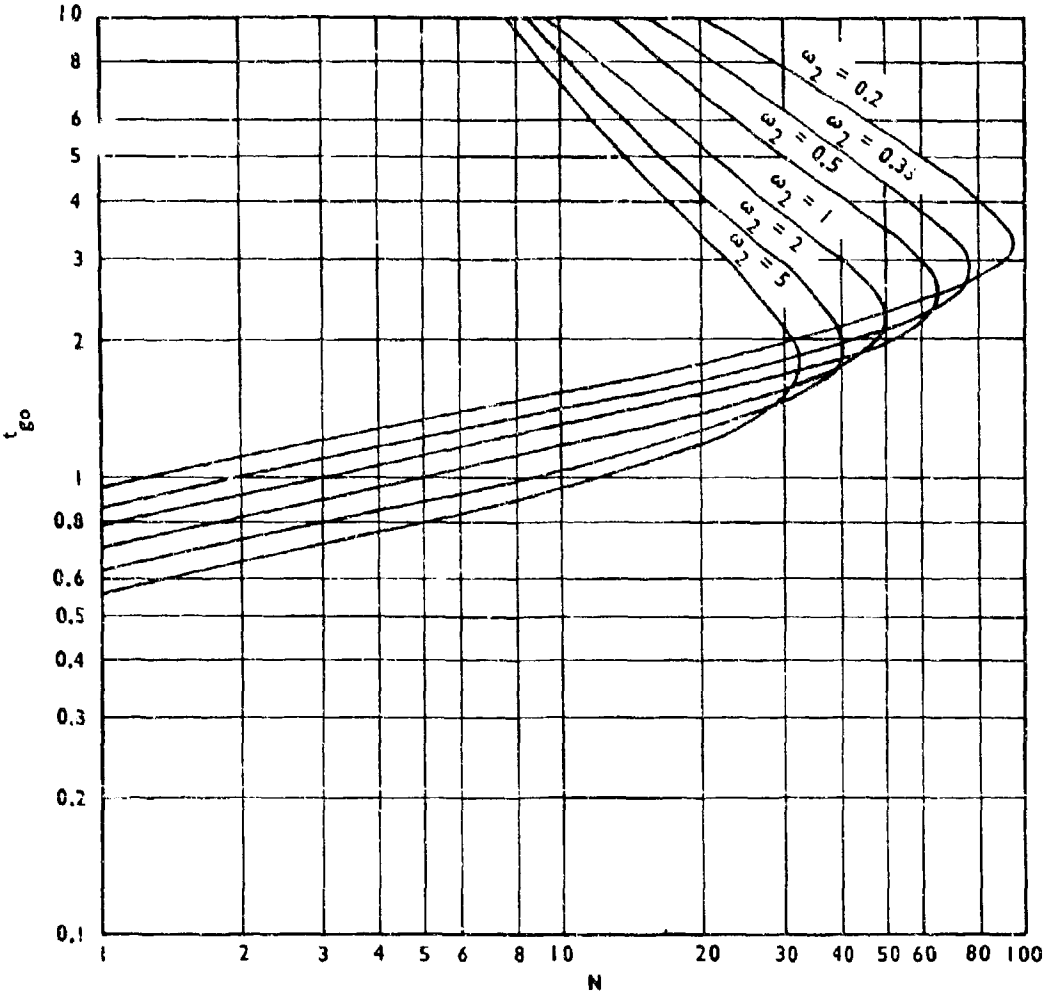

FIGURE B-7. N VERSUS t_{go} FOR $\omega_1 = 0.2$, $\lambda = 1$

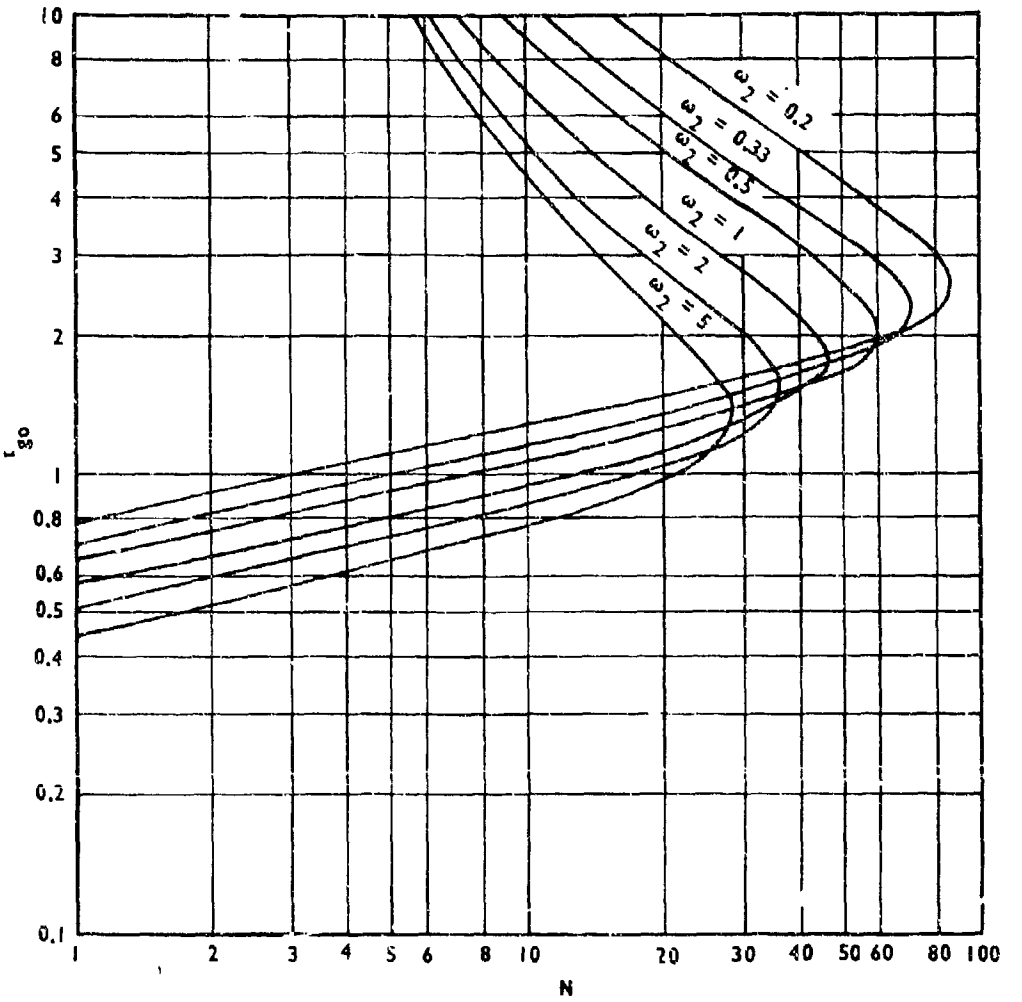

FIGURE B-8. N VERSUS t_{go} FOR $\omega_1 = 0.33$, $\lambda = 1$

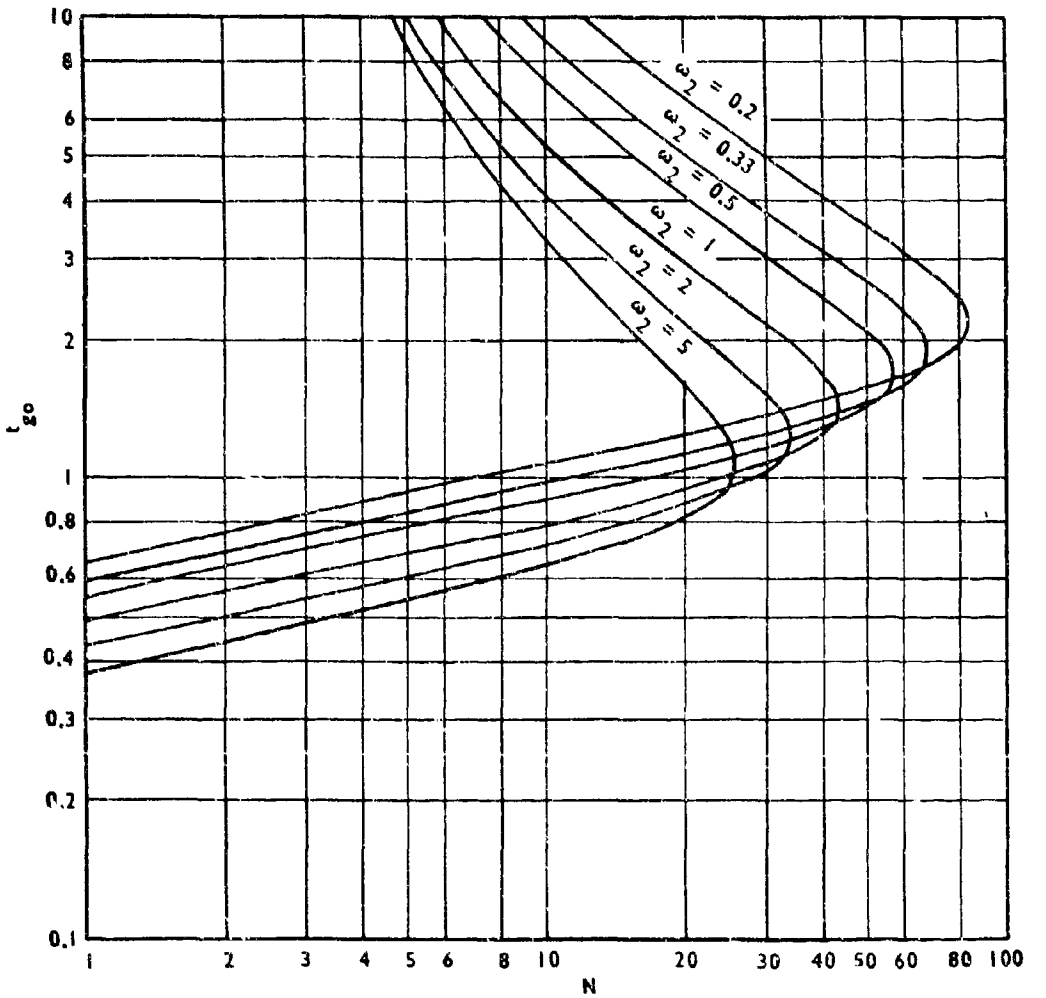

FIGURE B-9. N VERSUS t_{go} FOR $\omega_1 = 0.5$, $\lambda = 1$

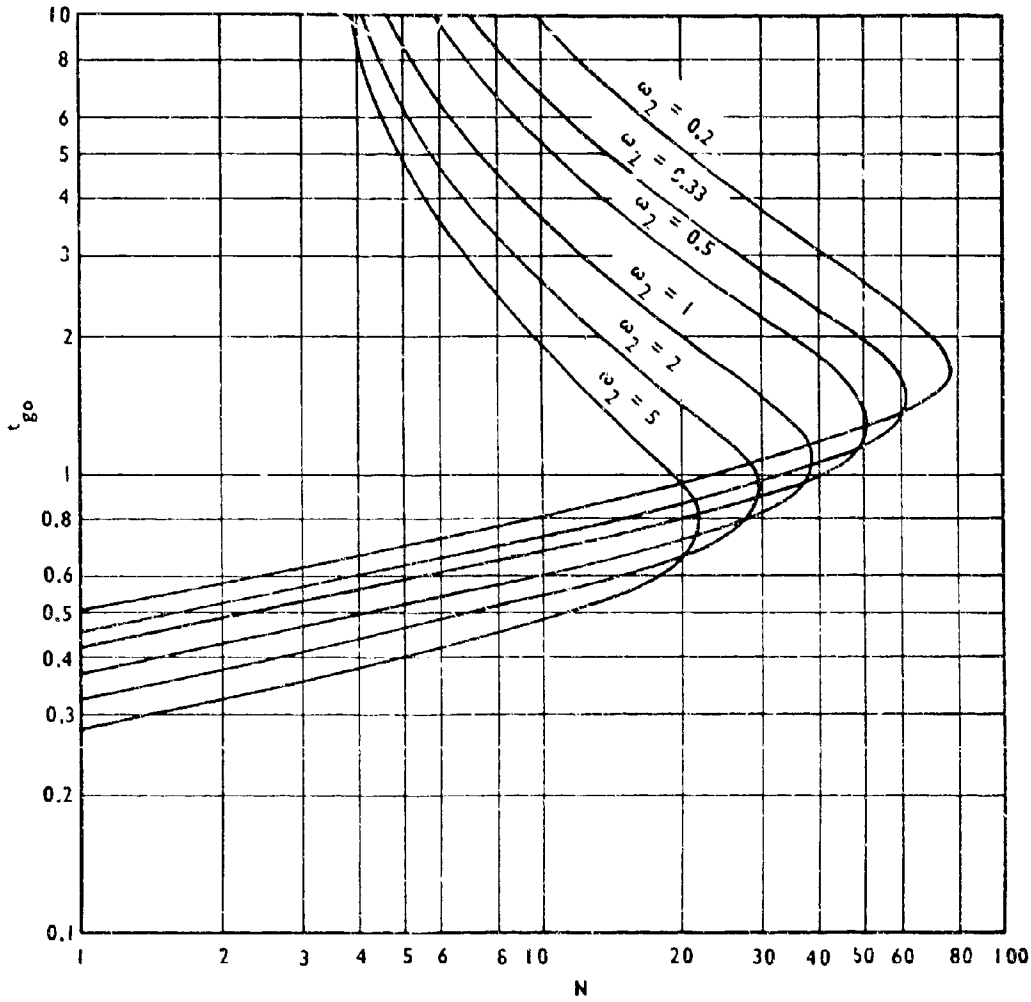

FIGURE B-10. N VERSUS t_{go} FOR $\omega_1 = 1$, $\lambda = 1$

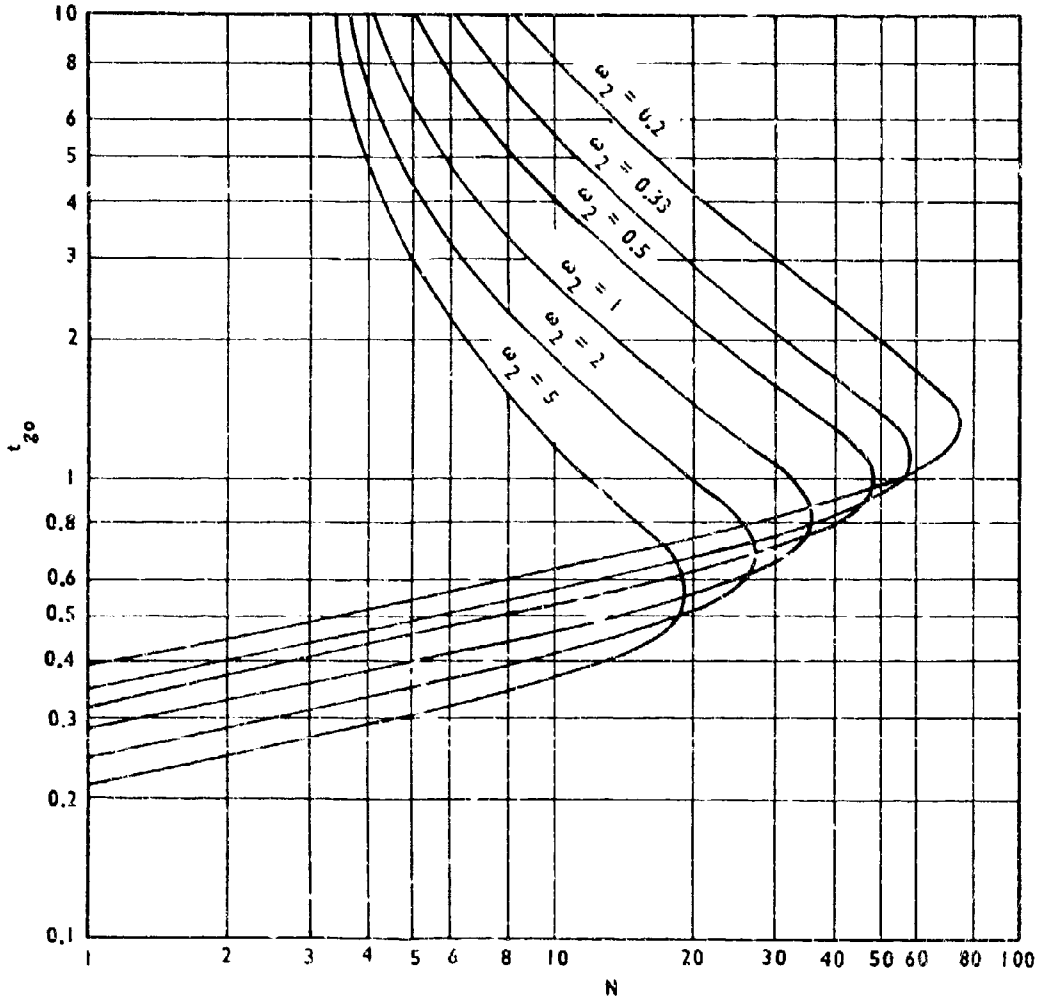

FIGURE B-11. N VERSUS t_{go} FOR $\omega_1 = 2$, $\lambda = 1$

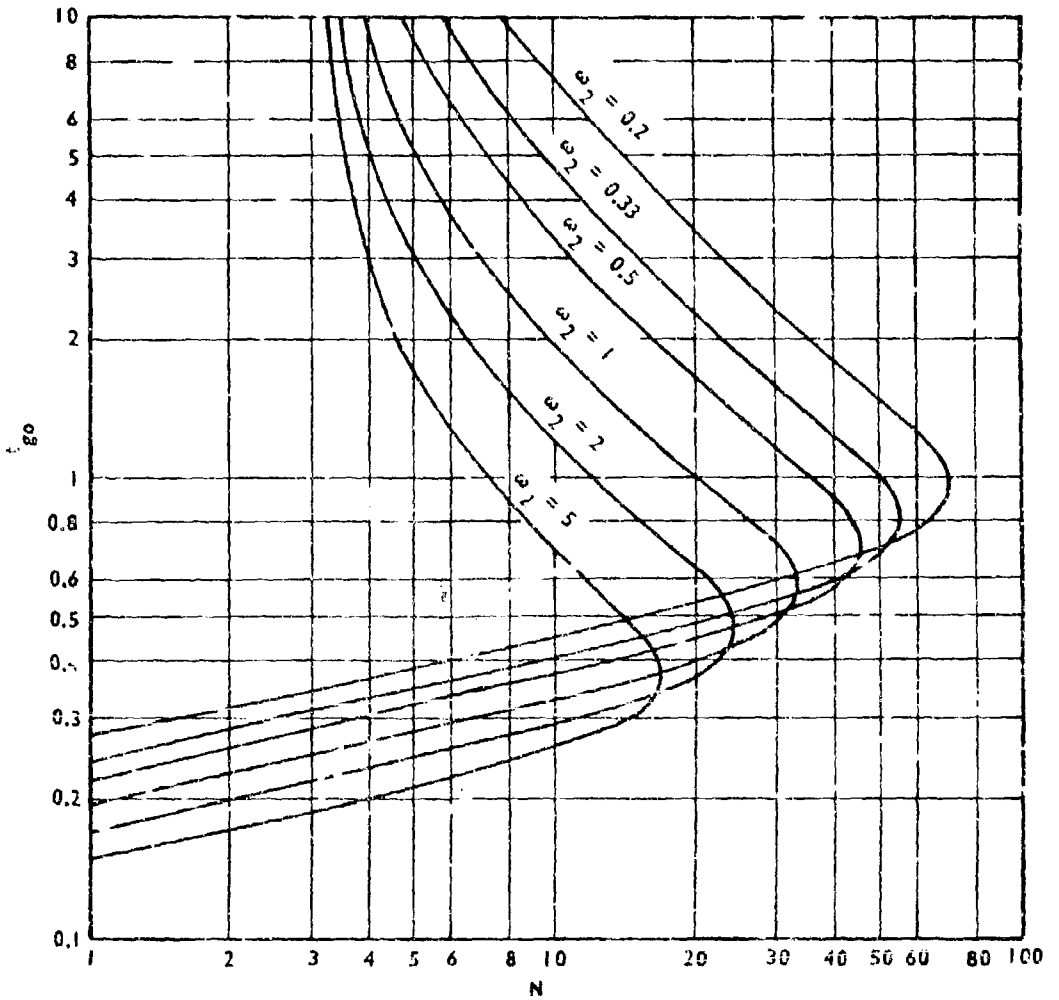

FIGURE B-12. N VERSUS t_{go} FOR $\omega_1 = 5$, $\lambda = 1$

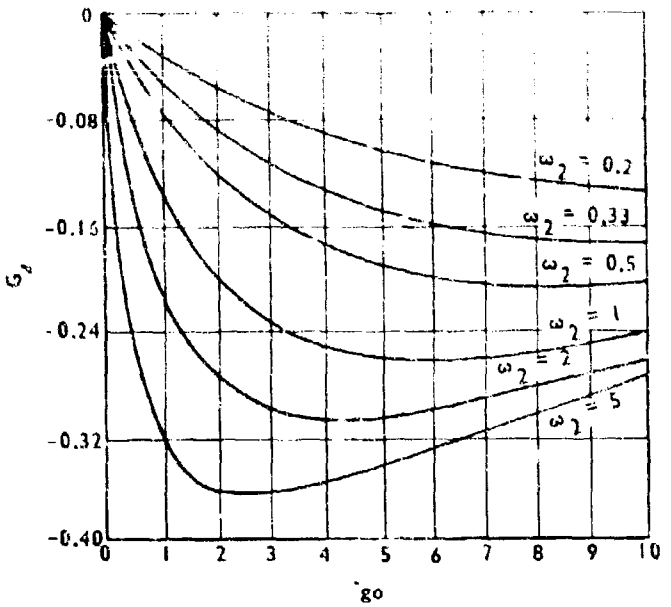

FIGURE B-13. G_4 VERSUS t_{go} FOR $\omega_1 = 0.2$

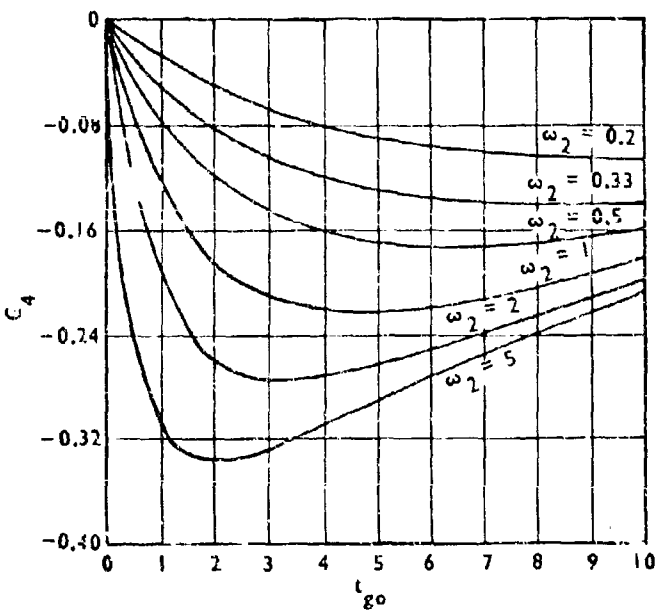

FIGURE B-14. G_4 VERSUS t_{go} FOR $\omega_1 = 0.33$

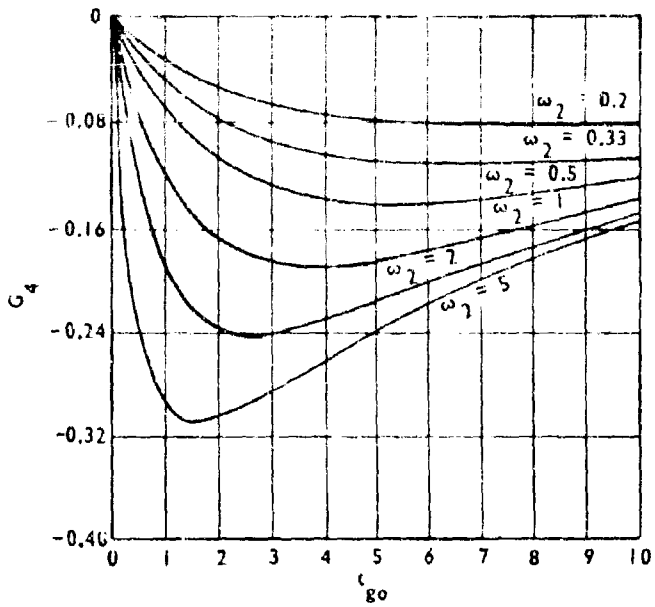

FIGURE B-15. G_4 VERSUS t_{go} FOR $\omega_1 = 0.5$

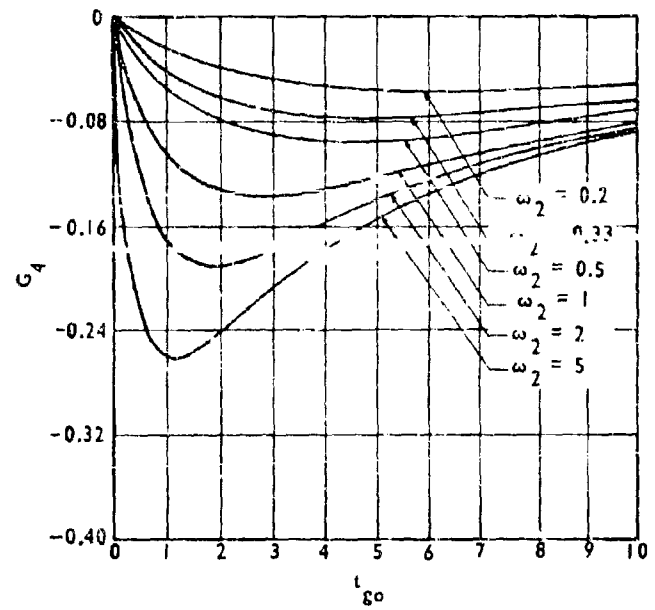

FIGURE B-16. G_4 VERSUS t_{go} FOR $\omega_1 = 1$

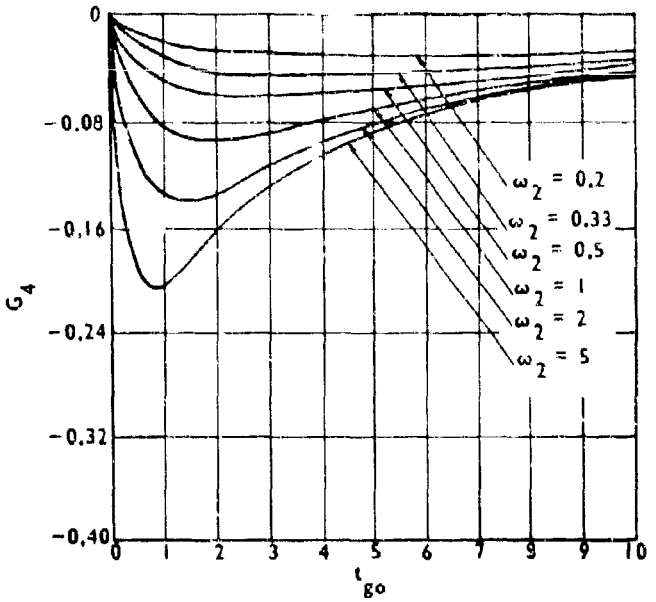

FIGURE B-17. G_4 VERSUS t_{go} FOR $\omega_1 = 2$

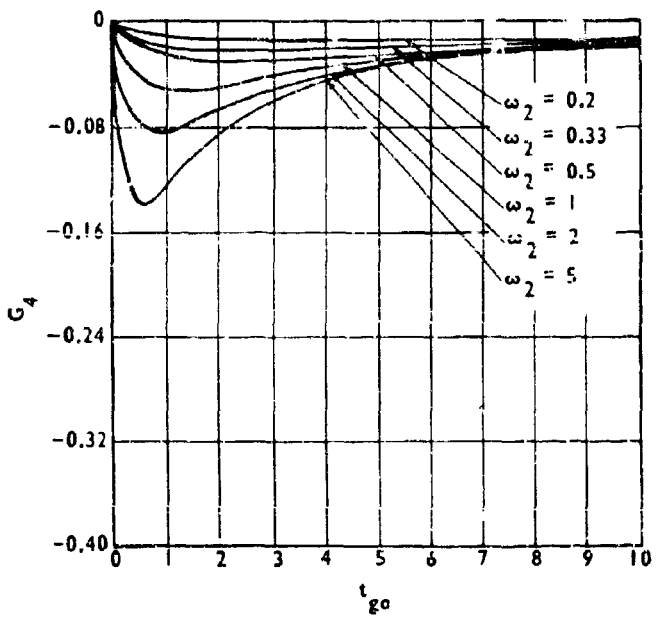

FIGURE B-18. G_4 VERSUS t_{go} FOR $\omega_1 = 5$

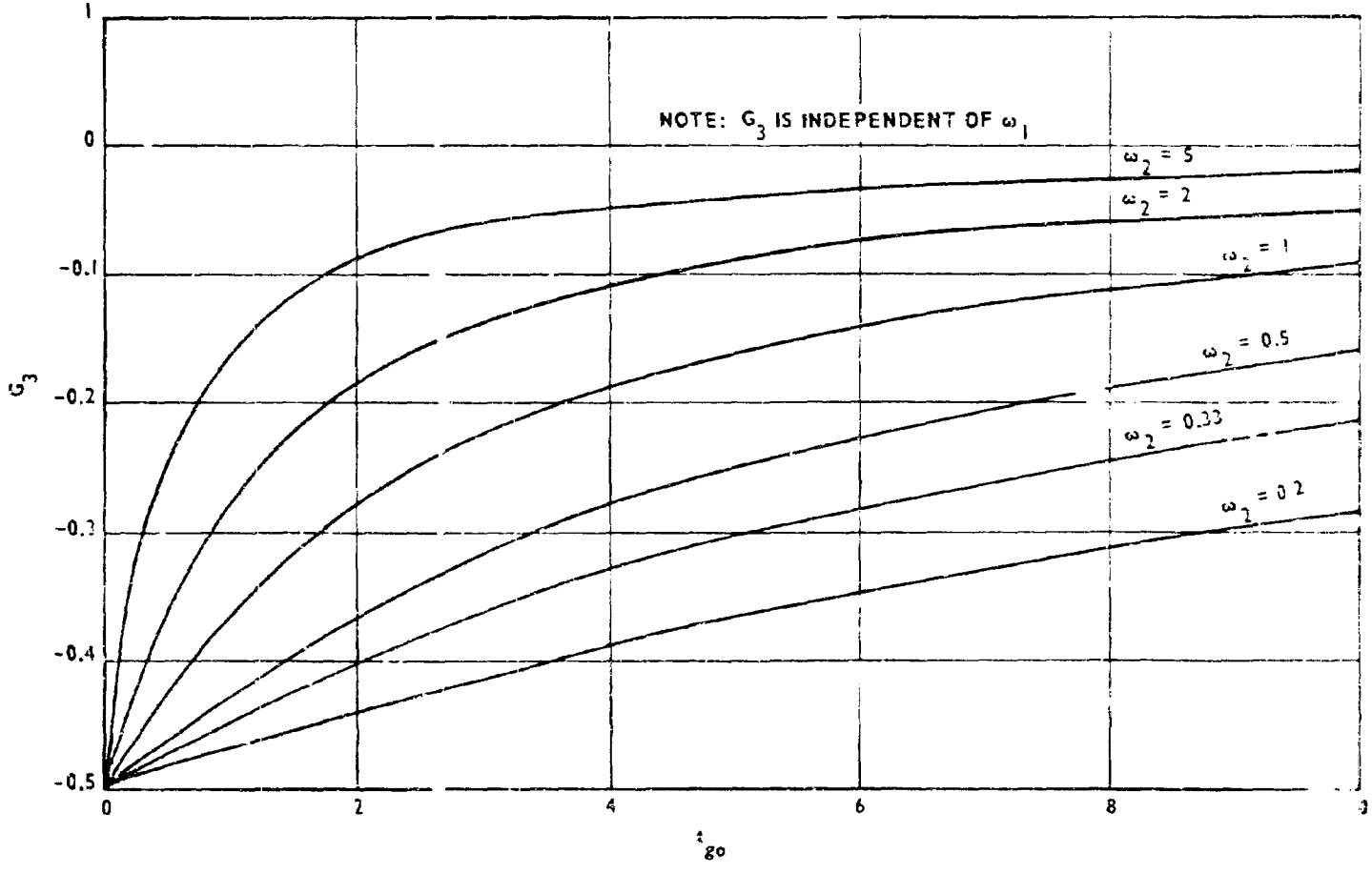

FIGURE B-19. G_3 VERSUS t_{go} FOR VARIOUS VALUES OF ω_2

REFERENCES

1. Ho, Y. C., Bryson, A. E., and Baron, S., "Differential Games and Optimal Pursuit-Evasion Strategies," IEEE Transactions on Automatic Control, AC-10, No. 4, October 1965, pp. 385-389.

2. Janus, J. P., Homing Guidance, Aerospace Corporation, El Segundo, California, December 1961, Report No. TOR-469(9990)-1.

3. Speyer, J., Optimal Control Theory and Biased Proportional Navigation, Raytheon Corporation, Bedford, Massachusetts, November 1967, Memo SAD-330.

4. Willems, G. C., Optimal Controllers for Homing Missiles, U. S. Army Missile Command, Redstone Arsenal, Alabama, September 1968, Report No. RE-TR-68-15.

5. Ogata, K., State Space Analysis of Control Systems, Englewood Cliffs, New Jersey, Prentice Hall, 1967, pp. 547-557.

6. Kalman, R. E., "A New Approach to Linear Filtering and Prediction Theory," Journal of Basic Engr., Trans. ASME, Ser. D, 82, March 1960, pp. 35-45.

7. Luenberger, D. G., "Observing the State of a Linear System," IEEE Trans. on Military Electronics, MIL-8, April 1964, pp. 74-80.

8. Bass, R. W., and Gura, I., "High Order System Design Via State-Space Considerations," 1965 Joint Automatic Control Conf. (preprint), pp. 311-318.

UNCLASSIFIED
Security Classification

DOCUMENT CONTROL DATA - R & D

(Security classification of title, body of abstract and indexing annotation must be entered when the overall report is classified)

1 ORIGINATING ACTIVITY (Corporate author) Advanced Sensors Laboratory Research and Engineering Directorate (Provisional) U. S. Army Missile Command Redstone Arsenal, Alabama 35809	2a. REPORT SECURITY CLASSIFICATION Unclassified 2b GROUP N/A

3 REPORT TITLE

OPTIMAL CONTROLLERS FOR HOMING MISSILES WITH TWO TIME CONSTANTS

4 DESCRIPTIVE NOTES (Type of report and inclusive dates)
Technical Report

5 AUTHOR(S) (First name, middle initial, last name)
G. C. Willems

6 REPORT DATE	7a. TOTAL NO OF PAGES	7b. NO OF REFS
9 October 1969	67	8

8a. CONTRACT OR GRANT NO	9a. ORIGINATOR'S REPORT NUMBER(S)
b. PROJECT NO (DA) 1M2623XXA204 c. AMC Management Structure Code No. 522C.11.146 d.	RE-TR-69-20 9b. OTHER REPORT NO'S) (Any other numbers that may be assigned this report) AD

10. DISTRIBUTION STATEMENT
This document is subject to special export controls and each transmittal to foreign governments or foreign nationals may be made only with prior approval of this Command, ATTN: AMSMI-RE.

11 SUPPLEMENTARY NOTES	12. SPONSORING MILITARY ACTIVITY
None	Same as No. 1

13 ABSTRACT

Optimum control theory is applied to develop a guidance law for homing missiles for which the airframe dynamics is not neglected. This work extends the applicability of the laws derived in a previous report to systems characterized by two time constants.

The effectiveness of the optimum controller thus derived is evaluated in an example by comparing it with classical proportional navigation. Additionally, extensive quantitative plots of the controller parameters are provided as an aid in specific designs.

DD FORM 1 NOV 68 1473 REPLACES DD FORM 1473, 1 JAN 64, WHICH IS OBSOLETE FOR ARMY USE.

UNCLASSIFIED
Security Classification

14 KEY WORDS	LINK A		LINK B		LINK C	
	ROLE	WT	ROLE	WT	ROLE	WT
Guidance						
Control						
Optimum control						
Proportional navigation						
Homing missiles						